

## **Chapter 3**

# **Production of bioflocculant CR4 and its biotechnological applications**

### **Chapter 3: Production of bioflocculant CR4 and its biotechnological applications**

Based on the fact that bioflocculants are ecofriendly and can be easily obtained from living organisms, they have become an inevitable product for large scale flocculation purpose. Due to the advantages of bioflocculants over chemical flocculants they have received prodigious awareness in the last decade (Okaiyeto *et al.*, 2016; Bakar *et al.*, 2021). The precedence of using amyloids is that these protein structures are highly resistant to physical and chemical denaturants such as heat, pH and presence of detergents.

In this chapter optimization of production conditions for bioflocculant CR4 were carried out. The bioflocculant production by bacteria is affected by several factors that include, carbon and nitrogen source and production conditions like pH and temperature, so also the growth of microalgae. Hence, the media optimization for *Scenedesmus* was also performed and optimized conditions were used for its flocculation studies. The *Scenedesmus* sp. flocculation process where *B. cereus* CR4 was applied also needed optimization. Finally, the application studies of nutrient removal by *Scenedesmus* from wastewater was conducted in the optimized condition determined in the preceding studies. Hence the studies were divided in five steps as follows:

- Medium optimization for bioflocculant CR4 production by *B. cereus* CR4 (section 3.1.1)
- Optimization of flocculation method of kaolin with purified protein (section 3.1.2)
- *Scenedesmus* sp. cultivation and optimization of media (section 3.1.3)
- Application of *B. cereus* CR4 in microalgal harvest (section 3.1.4)
- Application of *B. cereus* CR4 in harvest of *Scenedesmus* employed for nutrient removal from wastewater (section 3.1.5)

### **3.1 Materials and Methods**

#### **3.1.1 Media optimization for bioflocculant CR4 production by *B.cereus* CR4**

##### **3.1.1.1 Effect of temperature and pH on bioflocculant production by *B. cereus* CR4**

The influence of temperature and pH was determined by OFAT method. To study the effect of temperature on bioflocculant production by *B.cereus* CR4, a loopful of culture was inoculated into Luria broth and incubated at 37°C for 16hrs with 160RPM of agitation. 1% of the culture (0.4 OD<sub>600nm</sub>) was inoculated in 50ml Luria broth in 250ml flask. The flasks were incubated at different temperature ranging from 25°C, 30°C, 37°C, 40°C with 160RPM agitation. Flocculation activity was determined as described in chapter 2 (section 2.2.3) and the growth of bacteria was estimated by measuring optical density at 600nm. The temperature showing maximum flocculation was selected for further studies.

To study the effect of different pH on bioflocculant production by *B. cereus* CR4 the culture was first inoculated in Luria broth tubes and then 1% culture broth of 0.4 OD<sub>600nm</sub> was transferred to 50ml Luria broth (in 250ml flask) having pH viz. 4, 5, 7, 9, 10 and incubated at 37°C for 16hrs with 160RPM agitation. The bioflocculation activity was measured as described above. The growth of bacteria was estimated by measuring OD at 600nm. The buffers used to maintain the pH were 10mM of Acetate buffer (pH-4.0, 5.0), 10mM Phosphate buffer (pH- 7.0) and 10mM Tris buffer (pH- 9.0, 10.0).

##### **3.1.1.2 Plackett Burman design for screening of media components for bioflocculant production by *B. cereus* CR4**

The experimental design for the Plackett Burman analysis was generated by Design expert software (version 9.0). The basal medium for screening of nutrients using Plackett Burman analysis was 10mM Phosphate buffer saline where 1% nutrient namely Glucose, lactose, ammonium sulfate, manitol, yeast extract, tryptone, sucrose, sodium hydrogen phosphate, magnesium chloride, calcium chloride, peptone, urea, potassium chloride, sodium nitrate and beef extract were added (Table. 3.1). The table 3.4 depicts 20 experimental runs generated by the software and the results of the experiments. 1% *B. cereus* CR4 culture of 0.4

OD600nm was inoculated in 50ml Luria broth and grown for 16hrs at 37°C. Once cultivated, the culture broth was centrifuged and the bacterial pellet was resuspended in equal volume of saline. 1% of the resuspended cells were used as an inoculum for the flasks prepared previously for the Plackett Burman analysis. The flasks were incubated for 16hrs at 37°C and the flocculation activity was measured with 0.5% kaolin suspension, as described previously.

**Table 3. 1** Plackett Burman experimental design for analysis of bioflocculant production by *B.cereus* CR4

	Lactose	Glucose	NH4SO4	Manitol	Yeast extract	Tryptone	sucrose	Na2HPO4	MgCl2	CaCl2	Peptone	Urea	NaN03	Beef extract	Kcl	Dummy 1	Dummy 2	Dummy 3	Dummy 4
RUN	g/l	g/l	g/l	g/l	g/l	g/l	g/l	g/l	g/l	g/l	g/l	g/l	g/l	g/l	g/l	g/l	g/l	g/l	g/l
1	10	10	0	0	10	10	10	10	0	10	0	10	0	0	0	10	10	0	0
2	0	10	10	0	0	10	10	10	10	0	10	0	10	0	0	0	0	10	10
3	10	0	10	10	0	0	10	10	10	10	0	10	0	10	0	0	0	0	10
4	10	10	0	10	10	0	0	10	10	10	10	0	10	0	10	0	0	0	0
5	0	10	10	0	10	10	0	0	10	10	10	10	0	10	0	10	0	0	0
6	0	0	10	10	0	10	10	0	0	10	10	10	10	0	10	0	10	0	0
7	0	0	0	10	10	0	10	10	0	0	10	10	10	10	0	10	0	10	0
8	0	0	0	0	10	10	0	10	10	0	0	10	10	10	10	0	10	0	10
9	10	0	0	0	0	10	10	0	10	10	0	0	10	10	10	10	0	10	0
10	0	10	0	0	0	0	10	10	0	10	10	0	0	10	10	10	10	0	10
11	10	0	10	0	0	0	0	10	10	0	10	10	0	0	10	10	10	10	0
12	0	10	0	10	0	0	0	0	10	10	0	10	10	0	0	10	10	10	10
13	10	0	10	0	10	0	0	0	0	10	10	0	10	10	0	0	10	10	10
14	10	10	0	10	0	10	0	0	0	0	10	10	0	10	10	0	0	10	10
15	10	10	10	0	10	0	10	0	0	0	0	10	10	0	10	10	0	0	10
16	10	10	10	10	0	10	0	10	0	0	0	0	10	10	0	10	10	0	0
17	0	10	10	10	10	0	10	0	10	0	0	0	0	10	10	0	10	10	0
18	0	0	10	10	10	10	0	10	0	10	0	0	0	0	10	10	0	10	10
19	10	0	0	10	10	10	10	0	10	0	10	0	0	0	0	10	10	0	10
20	0	0	0	0	0	0	0	0	0	0	0	0	0	0	0	0	0	0	0

### 3.1.1.3 Media optimization using RSM for bioflocculant production by *B. cereus* CR4

The factors showing significant effect in bioflocculant production were selected by Plackett Burman analysis. Using Design expert software (version 9.0) various concentration of these

factors were selected and response surface methodology (RSM) was implemented for experimental analysis. The RSM method used was central composite design.

Inoculum were prepared by inoculating loopful of culture in 50ml Luria broth and incubating it at 37°C for 16hrs. The biomass was harvested by centrifugation at 8500g for 10mins and resuspended in equal volume of saline. 1% of resulting suspension at 0.4 OD<sub>600nm</sub> was then used to inoculate flasks prepared for response surface design and incubated at 37° C for 16 hours on a rotary shaker and flocculation activity and amyloid quantification were determined. Analysis and interpretation of results was done using Design expert software.

### **3.1.2 Optimization of flocculation method of kaolin with purified protein using CCD**

For the optimization of flocculation, the culture of *B. cereus* CR4 was grown at 37°C for 16 hrs and biomass was harvested by centrifugation at 8500g for 15 min. Purification of bioflocculant from the biomass was done as described in chapter 2 section 2.2.6. The purification process was repeated several times and pooled to get good amount of protein. The estimation of protein in the pooled sample was done by Folin Lowry method (Lowry et al., 1951).

Once the protein was purified 10ml of 0.5% kaolin was taken in different test tubes and flocculation was studied at different concentrations of protein (20, 40 and 60µg/ml) at pH 5, 7 and 9. Once mixed the kaolin suspension was vigorously vortexed and allowed to settle for 10 min. 1ml of the upper phase was taken in a separate tube and its optical density was measured at 595nm. Untreated Kaolin suspension was used as control.

For optimization of flocculation three factors viz. pH, CaCl<sub>2</sub> and amyloid concentration were selected to perform CCD experiment. The generation of response surface table of experimental design was done by Design expert software (version 9.0). The experimental runs were carried out according to design expert table. Once the results were obtained the experimental values were entered in the CCD table followed by computation of the mathematical equation by the software. After the mathematical equation was obtained the

response generated by the equation was compared with the actual experimental results and the comparison was demonstrated in the ANOVA table. The predicted response was then used to plot contour plots which represented graphical form for the optimal response.

### **3.1.3 *Scenedesmus* sp. cultivation and optimization of media**

*Scenedesmus* culture was provided by Dr. V. Sivasubramanian director of Phycospectrum Environmental Research Centre (PERC), Tamil Nadu. It was grown in media depicted in table 3.2. The microalgae was cultivated in three different media viz. Walne's, Bold's basal and BG11 media for 15 days at 30°C with 100RPM agitation under bright white light in respective. Once cultivated the culture was centrifuged at 8500g and dried in hot air oven at 65° for 12hrs. The dry weight of biomass was measured as estimate of growth. Based on the results obtained the factors present in the respective media were selected for Plackett Burman analysis.

**Table 3. 2** Different media used for the cultivation of *Scenedesmus*.

Walne's medium		Bold's basal medium		BG11 medium	
Component	amount mg%	Component	amount mg%	Component	amount mg%
NaNO3	100	NaNO3	2.5	NaNO3	150
ZnSO4	2	MgSO4	0.75	K2HPO4	4
CoCl2	2	NaCl	0.25	MgSO4	7.5
CuSO4	2	K2HPO4	0.75	CaCl2	3.6
FeCl3	1.3	KH2PO4	1.75	Na2CO3	2
MnCl2	0.36	CaCl2	0.25	H3BO3	286
H3BO3	33.6	ZnSO4	0.2	MnCl2	180
Na2HPO4	20	MnCl2	0.025	ZnSO4	22
		CuSO4	0.0375	CuSO4	8
		Co(NO3)2	0.0125	Co(NO3)2	5
		H3BO3	0.275		
		FeSO4	0.125		

#### **3.1.3.1 Plackett Burman design for screening of media components for growth of *Scenedesmus***

Based on the growth of *Scenedesmus* obtained in different media, the components of the respective media were selected for Plackett Burman screening. The salts used for the Plackett Burman analysis were: - NaNO<sub>3</sub>, K<sub>2</sub>HPO<sub>4</sub>, MgSO<sub>4</sub>, CaCl<sub>2</sub>, Na<sub>2</sub>CO<sub>3</sub>, FeCl<sub>3</sub>, ZnSO<sub>4</sub>, H<sub>3</sub>BO<sub>3</sub>

and trace metal elements. The table 3.3 represents the list of media components selected for the study. The Plackett Burman table was generated by Design Expert software (version 9.0) and the experimental runs were carried out accordingly. Once the experimental runs were over the effect of each factor was calculated by the statistical F test between the factor and the dummy variable.

### 3.1.3.2 Response surface methodology for media optimization for growth of *Scenedesmus*

The media components NaNO<sub>3</sub> and ZnSO<sub>4</sub> that gave significant microalgal growth in Plackett Burman design, were selected for central composite design. The experimental runs and data analysis for CCD was done by design expert software. Accordingly, 9 flasks containing different concentration of NaNO<sub>3</sub> and ZnSO<sub>4</sub> were prepared and inoculated with 10% of 0.8 OD750nm pre-grown algae.

**Table 3. 3** List of nutrients selected for Plackett Burman analysis for growth of *Scenedesmus* sp.

<b>Component</b>	<b>Amount (mg/100 ml)</b>
<b>NaNO<sub>3</sub></b>	150
<b>K<sub>2</sub>HPO<sub>4</sub></b>	4
<b>MgSO<sub>4</sub></b>	7.5
<b>CaCl<sub>2</sub></b>	3.6
<b>Na<sub>2</sub>CO<sub>3</sub></b>	2
<b>FeCl<sub>3</sub></b>	1.3
<b>ZnSO<sub>4</sub></b>	22
<b>H<sub>3</sub>BO<sub>3</sub></b>	286
<b><u>Trace metals</u></b>	
<b>CoCl<sub>2</sub></b>	2
<b>CuSO<sub>4</sub></b>	2
<b>Co(NO<sub>3</sub>)<sub>2</sub></b>	5
<b>MnCl<sub>2</sub></b>	0.36

The flasks were incubated at 30°C for 15 days with 100RPM for agitation. Once cultivated the biomass was harvested by centrifugation and dried in hot air oven at 65°C. The dry weight

of algal biomass was measured as a response and used to generate contour plots. The optimal region shown by the contour plot was selected and confirmed experimentally.

### **3.1.4 Application of *B. cereus* CR4 in microalgal harvest**

One of the important issues to be resolved in the applications with microalgae cultivation for biofuel productions is the need for efficient and cost-effective harvesting and processing of microalgae following cultivation. Hence amyloid producing *B. cereus* CR4 was studied for application in microalgae flocculation.

#### **3.1.4.1 Optimization of *Scenedesmus* sp. flocculation by *B. cereus* CR4 biomass using CCD**

*Bacillus* CR4 was used as a flocculation agent. A loopful of culture was inoculated in Luria broth in a test tube and incubated at 37°C for 16hrs with 160RPM shaking. 1% 0.4 OD<sub>600</sub> nm of this culture was inoculated in 50ml medium in Luria broth and incubated at 37°C for 16hrs with 160RPM shaking. Biomass was harvested by centrifugation at 8500g for 15 min and used at different cell densities in the experiment. Three factors viz Fe<sup>+3</sup> ions, pH and cell density of bacteria, required for flocculation were taken into account for optimization. The optimization was carried out with Design expert software (version 9.0). For the three selected factors the software generated 16 experimental runs with varying concentration of Fe<sup>+3</sup> ions, pH and cell density of bacteria. Flocculation was measured as described previously in chapter 2 section 2.2.3. Floc size of the aggregates was determined by measuring the settling velocity of the flocs. Once the contour plots were generated, the coordinates showing optimum flocculation activity was selected and verified experimentally. The floccules so generated were further collected and studied under bright field microscope

#### **3.1.4.2 Microscopy of flocculated microalgae**

The flocculated microalgae under optimized condition was taken on glass slide and observed under bright field microscope (Olympus CX43). The microalgae without addition of flocculant was used as a control.

#### **3.1.4.3 Factors affecting cell viability of *Scenedesmus* sp.**

The effect of pH and Fe<sup>+3</sup> on cell viability and growth of *Scenedesmus* was studied by using CCD as these factors cause chlorosis of algae. Using Design expert software (Version 9.0) different concentrations of Fe<sup>+3</sup> ions and pH were selected and experimental runs were designed. The culture of microalgae was pre-grown at 30°C for 15 days with 100RPM agitation. 10% of the microalgal culture was used as an inoculum for the flasks designed for CCD. Once inoculated the flasks were incubated at 30°C for 15 days with 100RPM agitation. The measurement of cell viability and growth was carried out as follows. The cell viability was measured by observing the algal cells under bright field microscope. The algal cells were taken on slide and stained with 1% methylene blue. The dead cells were stained blue while live cells remained green. The % of live cells were measured by estimating the number of live and dead cells respectively. The algal biomass was harvested by centrifugation and air dried in hot air oven at 65°C. The dry weight of biomass was measured as estimate of algal growth.

#### **3.1.4.4 Co-cultivation of *Bacillus* CR4 and *Scenedesmus* sp.**

With an aim to grow *Scenedesmus* in an aggregated form, co-cultivation strategy with *B. cereus* CR4 was employed. The growth of *B. cereus* CR4 was not supported by optimized BG11 medium used for *Scenedesmus* cultivation. In order to optimize the growth of both algae and bacteria during cocultivation two parameters viz concentration of glucose and inoculum of bacteria were taken into consideration and optimized by Central composite design using Design expert software (version 9.0).

#### **3.1.5 Application of *B. cereus* CR4 in harvest of *Scenedesmus* employed for nutrient removal from wastewater**

### **3.1.5.1 Bench scale studies**

10% inoculums with cell density 0.8OD at 750nm culture of *Scenedesmus* was inoculated in modified BG11 media and incubated at 30°C for 7 days under bright white light (1200 Lux) with 100RPM of agitation. The culture was harvested by centrifugation at 8500g for 15mins and the pellet was washed with sterile distilled water to remove traces of growth media. The pellet was resuspended in sterile distilled water and its optical density was adjusted to 0.8 at 750nm. This resuspended culture was then used to inoculate flasks containing 100ml of synthetic wastewater. Different % inoculum ranging from 2% to 10% was used in each flask. The flasks were incubated at 30°C for 7 days under white light (1200 Lux) with 100RPM agitation. The amount of residual nitrate and phosphate was measured by Brucine sulphate method (Follett and Ratcliff, 1963) and Fiske Subbarao method respectively (Fiske and Subbarow, 1925).

### **3.1.5.2 Batch reactor for nutrient removal from waste water**

Inorder to study the ability of *Scenedesmus* to remove phosphate and nitrates from waste water, a glass batch reactor with dimensions 12 inch x 12 inch x 10 inch used. The culture of *Scenedesmus* was cultivated in 100ml of optimized BG11 media for 7 days at 30°C with intense white light. Once the culture was grown the biomass was harvested by centrifugation and the pellet was washed with sterile distilled water to remove traces of previous media. The optical density (OD 750nm) of the harvested biomass was adjusted to 0.8 using sterile distilled water. 10% of the algal suspension was used as an inoculum for batch reactor filled with 5l of synthetic waste water. An aliquot of sample from the reactor was taken at an interval of 24hrs for 10 days followed by estimation of phosphate and nitrate in it. The reactor was operated in non sterile conditions in order to replicate the natural environment.

### **3.1.5.3 Preparation of bioflocculant for continuous reactor**

The culture of *B. cereus* CR4 was cultivated in TY broth at 37°C, till the OD (600nm) reaches 0.8. The biomass was harvested by centrifugation and resuspended in 1/10<sup>th</sup> volume of

distilled water. The harvested biomass was further mixed with 156 mg of  $\text{FeCl}_3$  and used as a flocculant for continuous reactor.

#### **3.1.5.4 Continuous reactor for nutrient removal from wastewater**

The batch reactor described above was modified to work as a continuous reactor. The continuous reactor had an overhead tank which contained synthetic waste water and an outlet system to drain the treated water. The culture of *Scenedesmus* was pre grown in modified BG11 media for 7 days at 30°C. The cultivated biomass was harvested by centrifugation at 8500g for 15mins. The biomass obtained in the pellet was washed several times with distilled water and re suspended to get final optical density (OD 750nm) to 0.8. Once the desired optical density was adjusted 10% of the culture was used as an inoculum for the continuous reactor containing 6.4L of synthetic waste water. The outflow of the reactor was connected to a flocculation tank that had an inlet of 18mg%  $\text{FeCl}_3$ . Once the algal floccules settled the supernatant was collected and subjected for nitrate and phosphate analysis. The reactor was operated at various flow rates ranging from 1 ml/min, 2 ml/min, 4.5 ml/min, 6 ml/min and 8 ml/min.

#### **3.1.5.5 Optimization of *Scenedesmus* sp. flocculation in continuous reactor**

The RSM method was designed for various flow rates of continuous reactor and bioflocculant mixing for efficient flocculation of microalgae after removal of nitrate and phosphate. The design was constructed using Design expert software (version 9.0) and the flow rates of reactor and bioflocculant was designed accordingly. The outflow from the reactor was mixed with bioflocculant producing *B.cereus* CR4 biomass in 200ml plastic beaker placed on magnetic stirrer with 100RPM of agitation. The outflow from the flocculation beaker was collected in a settling tank. The flocs of microalgae were allowed to settle for 1hr. The optical density of the upper phase was measured at 750nm and the % flocculation of microalgae was calculated. The flocculation values obtained at various flow rates were entered in the software to generate a mathematical equation for predicting the optimal flocculation of microalgae during continuous treatment. Once predicted the optimal results were confirmed experimentally at respective flow rates of reactor and bioflocculant.

#### **3.1.5.6 Estimation of Nitrate**

Nitrate estimation was carried out by Brucine sulphate method. For determination of nitrate, 2 mL of sample (with appropriate dilutions) was treated with 2 mL conc H<sub>2</sub>SO<sub>4</sub>. The mixture is cooled at 4°C in ice for 15mins and allowed to reach at room temperature for another 15mins. The samples were then subjected to heating to 90-95°C for 20 min followed by addition of 0.1 mL Brucine sulphate. The optical density was taken at 410 nm after cooling. The amount of nitrate so estimated was directly proportional to the optical density that was measured. This information was then used to plot standard graph for estimation of unknown nitrate concentration (Follett and Ratcliff, 1963).

#### **3.1.5.7 Estimation of phosphate**

Phosphate estimation was carried out by Fiske Subbarao Method. For determination of phosphate, 860µl of sample (with appropriate dilutions) was treated with 100µl Ammonium Molybdate and 40µl ANSA (Amino Naphthol sulphonic acid) reagent. The mixture was allowed to remain at room temperature for 5 min and the optical density was measured at 660 nm. A standard graph was plotted for estimation of unknown phosphate concentration (Fiske and Subbarow, 1925).

### **3.2 Results and Discussion**

#### **3.2.1 Media optimization for bioflocculant CR4 production by *B.cereus* CR4**

##### **3.2.1.1 Effect of temperature on bioflocculant CR4 production**

Temperature has a major effect on the activity of enzymes present in the cell which in turn affects the amount of bioflocculant production. For most of the bacteria the optimum temperature ranges from 30°C to 37°C. Hence the effect of different temperatures from 25°C, 30°C, 37°C, 40°C was studied on bioflocculant production by *B. cereus* CR4. The average flocculation observed at 37°C was 73.4% followed by 65.3% at 30°C. On increasing the incubation temperature at 40°C the flocculation activity sharply decreased by 53.2%,

demonstrating only 21.5% activity (Figure. 3.1). This observation was supported by the fact that most of the bioflocculant producing *Bacillus* species have an optimum growth temperature of 37°C. Xiong *et al.*, (2010) have reported bioflocculant producing *Bacillus lichiniiformis* that exhibits its maximum flocculation activity and growth at 37°C. Upon increasing the temperature from 37°C to 40°C there occurs complete loss in bioflocculant production. Based on this certitude optimum temperature of 37°C was selected for *B. cereus* CR4 for further studies.

### 3.2.1.2 Effect of pH on bioflocculant production

Apart from temperature, pH also has a significant role on metabolism. When the effect of different pH ranging from 4, 5, 7, 9, 10 was studied on bioflocculant production the average % flocculation observed was 63.9% for pH 5, 7 and 9 with no statistical difference (Figure. 3.2). The extreme pH values pH 4 and 10 showed 31.5% and 35% flocculation respectively. On a similar note, most of the *Bacillus* species have exemplified optimum pH of 7.0 for its growth.

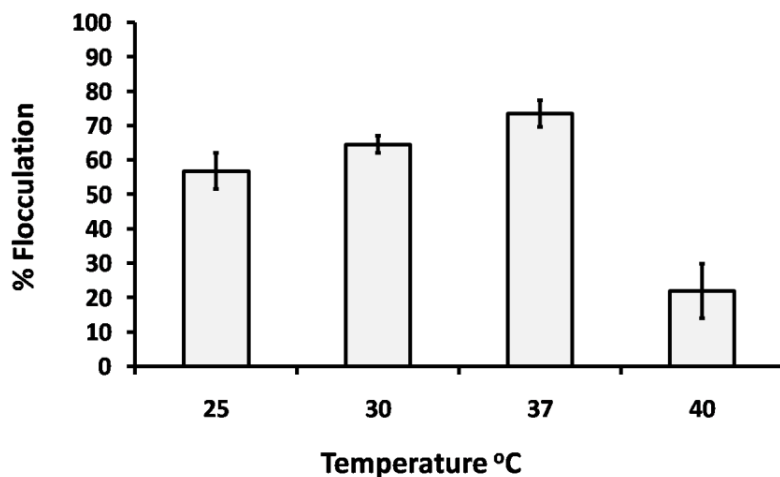


**Figure 3. 1** Effect of Temperature on bioflocculant CR4 production by *B. cereus* CR4.

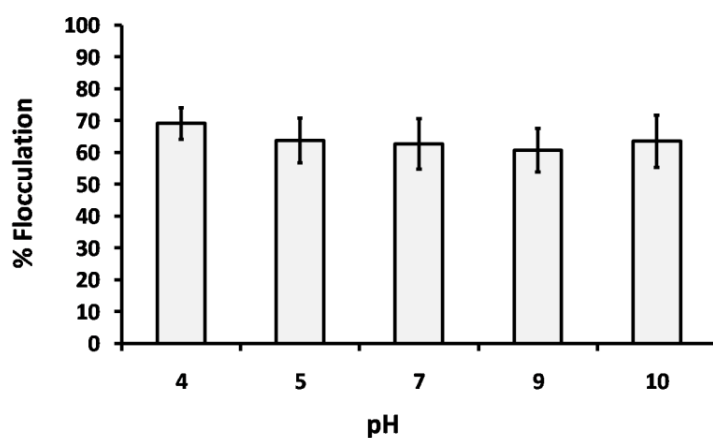


**Figure 3. 2** Effect of pH on bioflocculant production by *B. cereus* CR4.

### 3.2.1.3 Plackett Burman analysis for bioflocculant CR4 production.

The media used for the growth of bioflocculant producing *Bacillus cereus* CR4 have several components. In order to scrutinize the role of each nutrients on bioflocculant production the Plackett Burman analysis method was selected. Plackett Burman analysis is one of the widely used statistical methods used for the assortment of nutrient sources with profound effect on production of coveted biomolecule as well as growth. The method involves measurement of desired response by ascribing high and low concentrations of selected nutrients. The statistically significant variables are selected on the basis of F test. In this study effect of different nutrient sources (Carbon source: Glucose, Maltose, Lactose, Mannitol, Sucrose, Fructose, Xylose, Starch. Nitrogen sources: Yeast extract, Tryptone, Peptone, Beef extract) was studied on bioflocculant production (Table. 3.4). The high and low attributes for each nutrient source was designated using Design expert Software (Version 9.0). The bioflocculation activity was measured as an experimental response (Table. 3.4). The maximum flocculation activity of 75.3% was demonstrated by Run 6, followed by 65.1% of Run 8 and 58.5% of Run 11. The response due to each variable (nutrient) was compared with the dummy variable and the ensuing F ratio was calculated. The critical value was determined using statistical F table.

**Table 3. 4** Plackett Burman design and analysis for bioflocculant production by *B.cereus* CR4

RUN	Lactose g/l	Glucose g/l	NH4SO4 g/l	Manhitol g/l	Yeast extract g/l	Tryptone g/l	sucrose g/l	Na2HPO4 g/l	MgCl2 g/l	CaCl2 g/l	Peptpne g/l	Urea g/l	NaN03 g/l	Beef extract g/l	Kcl g/l	Dummy1 g/l	Dummy2 g/l	Dummy3 g/l	Dummy4 g/l	Flocculation %
1	10	10	0	0	10	10	10	10	0	10	0	10	0	0	0	10	10	0	0	55.6
2	0	10	10	0	0	10	10	10	10	0	10	0	10	0	0	0	0	10	10	25.3
3	10	0	10	10	0	0	10	10	10	10	0	10	0	10	0	0	0	0	10	34.8
4	10	10	0	10	10	0	0	10	10	10	10	0	10	0	10	0	0	0	0	5.1
5	0	10	10	0	10	10	0	0	10	10	10	10	0	10	0	10	0	0	0	55.1
6	0	0	10	10	0	10	10	0	0	10	10	10	10	0	10	0	10	0	0	75.3
7	0	0	0	10	10	0	10	10	0	0	10	10	10	10	0	10	0	10	0	10.2
8	0	0	0	0	10	10	0	10	10	0	0	10	10	10	10	0	10	0	10	65.1
9	10	0	0	0	0	10	10	0	10	10	0	0	10	10	10	10	0	10	0	52.7
10	0	10	0	0	0	0	10	10	0	10	10	0	0	10	10	10	10	0	10	55.3
11	10	0	10	0	0	0	0	10	10	0	10	10	0	0	10	10	10	10	0	58.5
12	0	10	0	10	0	0	0	0	10	10	0	10	10	0	0	10	10	10	10	40.2
13	10	0	10	0	10	0	0	0	0	10	10	0	10	10	0	0	10	10	10	12.5
14	10	10	0	10	0	10	0	0	0	0	10	10	0	10	10	0	0	10	10	42.3
15	10	10	10	0	10	0	10	0	0	0	0	10	10	0	10	10	0	0	10	45.6
16	10	10	10	10	0	10	0	10	0	0	0	0	10	10	0	10	10	0	0	41.2
17	0	10	10	10	10	0	10	0	10	0	0	0	0	10	10	0	10	10	0	35.3
18	0	0	10	10	10	10	0	10	0	10	0	0	0	0	10	10	0	10	10	55.4
19	10	0	0	10	10	10	10	0	10	0	10	0	0	0	0	10	10	0	10	25.6
20	0	0	0	0	0	0	0	0	0	0	0	0	0	0	0	0	0	0	0	5.1

The critical value determined by F table was 2.94, indicating that any ratio (of selected variable) above 2.94 will be statistically significant in its contribution for bioflocculant production. The F score for each variable has been elaborated in the table 3.5. Based on the reckoning of F score three nutrient factors viz. yeast extract, tryptone and lactose demonstrated the F ratio of 13.67, 7.23 and 4.51 respectively. On the basis of these results, it is concluded that yeast extract, tryptone and lactose played a consolidated role in bioflocculant production.

Yeast extract and tryptone are considered as nitrogen rich source of nutrient for the growth of bacteria. As the amyloid bioflocculant produced by *B. cereus* CR4 is made up of protein

and produced in logarithmic growth phase, it can be said that the nitrogen rich source significantly supports the bioflocculant production.

Besides yeast extract and tryptone, lactose showed a prominent role in bioflocculant production. The noteworthy role of lactose in the production of amyloid bioflocculant can be braced by the fact that biofilms of *B. cereus* CR4 are found wide spread in pile lines of dairy industries. These biofilms act as a major factor in deteriorating the quality of dairy products and consequential economic loss. Lactose which is common constituent of milk has been reported to increase quorum sensing AI2 production which sequentially upregulate TasA gene which codes for extracellular amyloid fibres resulting in cell aggregation and biofilm formation by the producing bacteria (Duanis-Assaf *et al.*, 2016).

**Table 3. 5** F test for Plackett Burman analysis of the optimization of media for bioflocculant production by *B.cereus* CR4.

<b>Factors</b>	<b>Variance</b>	<b>F ratio</b>
<b>Lactose</b>	911.25	<b>4.51</b>
<b>Glucose</b>	76.05	<b>0.37</b>
<b>NH4SO4</b>	84.05	<b>0.41</b>
<b>Manittol</b>	186.05	<b>0.92</b>
<b>Yeast extract</b>	2761.25	<b>13.67</b>
<b>Tryptone</b>	1462.05	<b>7.23</b>
<b>sucrose</b>	84.05	<b>0.41</b>
<b>Na2HPO4</b>	84.05	<b>0.41</b>
<b>MgCl2</b>	14.45	<b>0.07</b>
<b>CaCl2</b>	238.05	<b>1.17</b>
<b>Peptpne</b>	266.45	<b>1.31</b>
<b>Urea</b>	470.45	<b>2.32</b>
<b>NaNO3</b>	68.45	<b>0.33</b>
<b>Beef extract</b>	174.05	<b>0.86</b>
<b>Kcl</b>	8.45	<b>0.04</b>
<b>Dummy 1</b>	6.05	
<b>Dummy 2</b>	61.25	
<b>Dummy 3</b>	732.05	

#### **3.2.1.4 Optimization of bioflocculant production by Response surface methodology**

Optimization involves the use of various factors at different concentration and monitoring the resultant response. The response surface methodology involves the use of experimental data to generate mathematical equation for the prediction of optimal response value. The response of each level is measured experimentally and the results are computed using a software (Design expert) to generate mathematical equation for predicting the optimal values. Once the levels for each factor were decided, the response for experimental runs were generated.

The Plackett Burman analysis demonstrated the role of three important nutrient factors that had impact on bioflocculant production. These three factors were lactose, tryptone and yeast extract. The response surface methodology (central composite design) was used for finding the optimal concentrations of Lactose, Yeast extract and Tryptone for maximum bioflocculant production. The experimental runs for the central composite design were generated using Design expert software (Version 9.0) by inputting various concentration ranges for various factors, in the software. Experiments were carried out for each run and the results so obtained are indicated in Table. 3.6. The experimental results were analyzed by the software to develop a mathematical equation that can predict the response at different levels of selected nutrients. The accuracy of the equation was examined by ANOVA analysis of the model and lack of fit values (Table. 3.7).

In order to verify significance of the mathematical equation derived in terms of lactose, yeast extract and tryptone, the p-value for the model was checked in the ANOVA table (Table. 3.7). The p-value calculated for the model was 0.0116 which indicated that there was only 1.116% chance for the predicted value to statistically deviate from the experimental value. The p-value for each factor viz. lactose, yeast extract and tryptone were 0.019, 0.043 and 0.001 respectively. As the p-value of each selected nutrient source were less than 0.05 it shows that all selected factors had significant contribution in bioflocculant production. These p-value for each factor also vouch for the fact that the results obtained in the Plackett Burmann analysis were veracious.

After scrupulous analysis of the ANOVA table for each factor, the graph of predicted vs actual was analyzed for final confirmation of the mathematical equation (Figure. 3.3). The points on the predicted vs actual graph falls on the straight line which indicated that the response generated by the mathematical equation and experimental response are similar. Hence counter plots were generated to perceive their respective concentration that capitulate maximum bioflocculant production.

**Table 3. 6** Experimental results of media optimization for bioflocculant production by *B.cereus* CR4 using central composite design

Lactose(%)	YE(%)	Tryptone(%)	Flocculation(%)	Amyloid(ug/mg Biomass)
0.2	0.2	0.2	11.8	0.002
0.8	0.2	0.2	12.3	0.01
0.2	0.8	0.2	41.6	0.44
0.8	0.8	0.2	39.6	0.12
0.2	0.2	0.8	67.5	0.78
0.8	0.2	0.8	55.2	0.57
0.2	0.8	0.8	88.9	1.16
0.8	0.8	0.8	50.51	0.49
0.0	0.5	0.5	70.1	0.88
1.0	0.5	0.5	30.1	0.077
0.5	0.0	0.5	35	0.102
0.5	1.0	0.5	48.2	0.53
0.5	0.5	0.0	34.2	0.091
0.5	0.5	1.0	65.1	0.68
0.5	0.5	0.5	76.3	0.71
0.5	0.5	0.5	73.3	0.61

The role of selected nutrient source, lactose, yeast extract and tryptone can be discerned in figure 3.4. According to the figure 3.3, increase in yeast extract from 0.2 to 0.65% increases the bioflocculant production. Whereas low concentration of lactose (0.25%) favours the production of bioflocculant. The increase in lactose concentration from 0.3 to 0.8% has opposite effect on bioflocculant production.

When the effect of yeast extract and tryptone was analyzed (figure 3.4) it was found that the increase in tryptone from 0.2 to 0.7% and increase in yeast extract from 0.2 to 0.6% showed flocculation activity of 81.5%. On analysing the effect of yeast extract and tryptone at constant concentration of lactose (0.25%) it was observed that 0.5% yeast extract and 0.7% tryptone demonstrates an optimum flocculation activity of 88.3%. This was later confirmed experimentally at the respective concentrations of tryptone, yeast extract and lactose which showed 89.2% flocculation activity.

**Table 3. 7** ANOVA analysis for media optimization for bioflocculant production by *B.cereus* CR4 using CCD.

Source	Sum of Squares	df	Mean Square	F-Value	P value
Model	7023.72	9	780.41	7.52	0.0116
A-Lactose	1045.15	1	1045.15	10.07	0.0192
B-Yeast Extract	674.82	1	674.82	6.50	0.0435
C-Tryptone	3191.35	1	3191.35	30.75	0.0015
AB	102.24	1	102.24	0.99	0.3593
AC	302.58	1	302.58	2.92	0.1386
BC	204.02	1	204.02	1.97	0.2105
A <sup>2</sup>	688.24	1	688.24	6.63	0.0420
B <sup>2</sup>	1251.83	1	1251.83	12.06	0.0133
C <sup>2</sup>	713.88	1	713.88	6.88	0.0395
Residual	622.77	6	103.79		
Lack of Fit	618.27	5	123.65	27.48	0.1438



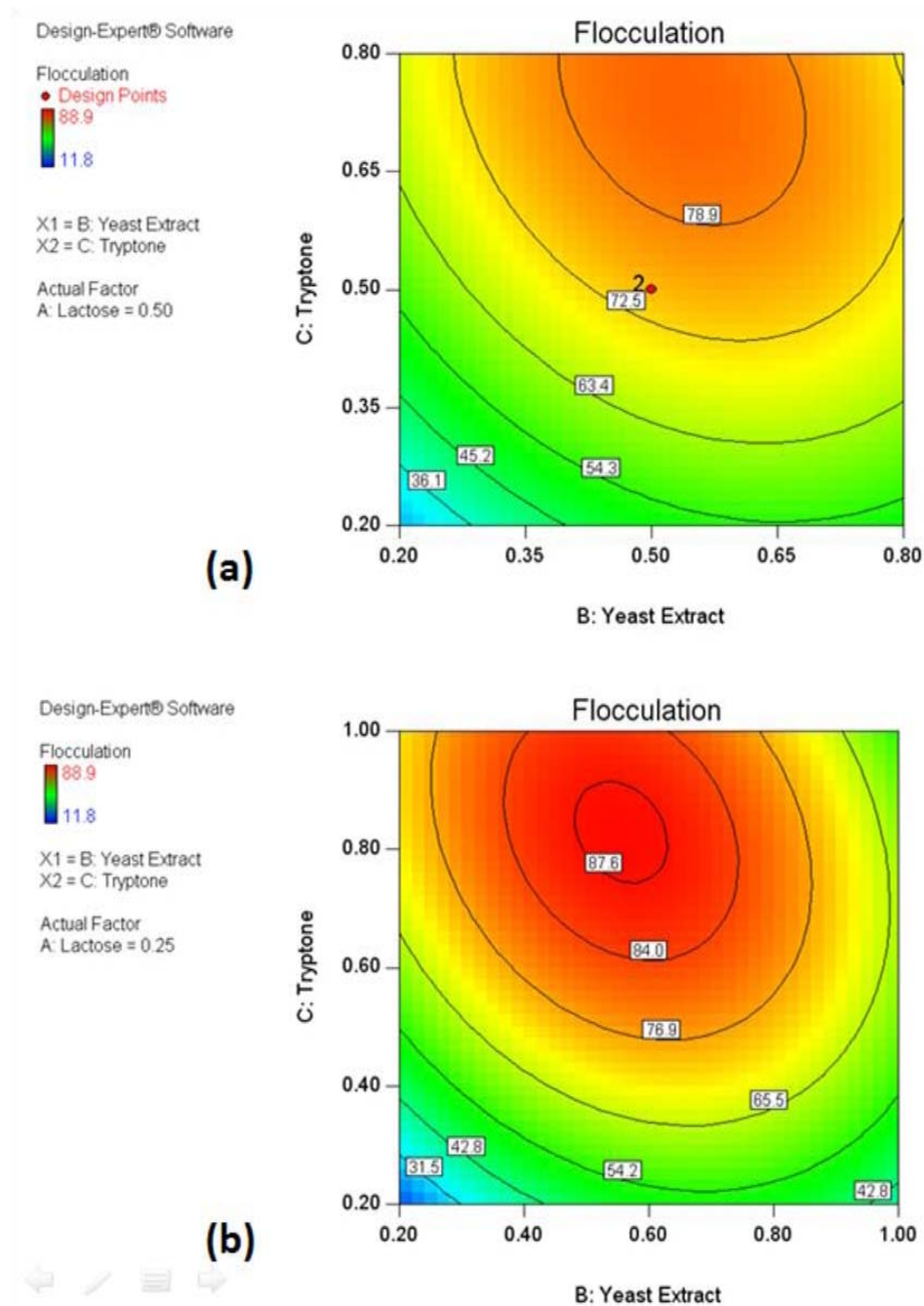


**Figure 3. 4** CCD for optimization of lactose, yeast extract and tryptone for bioflocculant production by *B. cereus* CR4. a) Effect of tryptone and yeast extract on bioflocculant production. b) Effect of tryptone and yeast extract on bioflocculant production.

### **3.2.2 Optimization of flocculation method of kaolin with purified amyloid bioflocculant protein using CCD**

#### **3.2.2.1 Effect of pH and amyloid concentration on flocculation of kaolin**

The purified amyloid protein from SDS agarose demonstrated flocculation activity (Figure. 3.5). The pH and concentration of bioflocculant governs the aggregation phenomenon that leads to flocculation. pH determines the net charge on the bioflocculant which in turn determines the interaction of bioflocculant with the suspended kaolin particles. In case of purified amyloid protein *B. cereus* CR4, 61% flocculation activity was observed at an acidic pH of 5 and 60  $\mu\text{g/ml}$  amyloid concentration (Figure. 3.5). Exclusively proteinaceous bioflocculant as in the case of *B. cereus* CR4 has not been earlier reported from *Bacillus* sp. Amyloid protein nature affords biodegradability as well as robustness to the bioflocculant for industrial use. The results here clearly demonstrate that the amyloid protein produced by *B. cereus* CR4 has flocculation activity. The bioflocculant produced by *B. cereus* CR4, exploits the unique sturdy nature of amyloid to confront harsh physical and chemical stress.

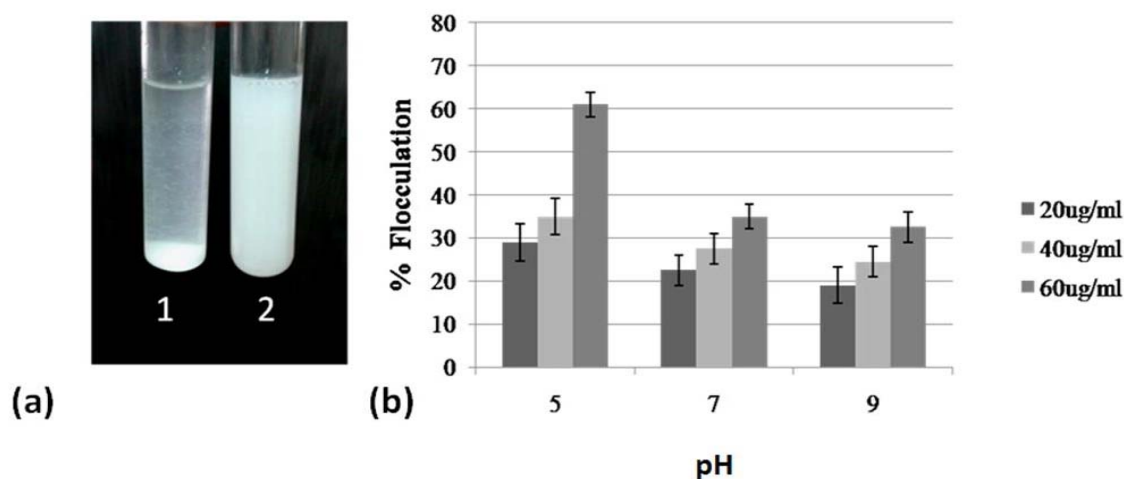


**Figure 3. 5** Effect of pH and amyloid addition on flocculation of kaolin. a) Tube 1. flocculated kaolin (at pH 5 and 60 $\mu\text{g/ml}$  amyloid concentration). Tube 2-control (kaolin + d/w). b) Effect of pH and amyloid concentration on flocculation of kaolin.

### **3.2.2.2 Optimization of flocculation of kaolin with purified bioflocculant CR4 by response surface methodology.**

The turbid waste water from domestic, industrial and agricultural effluents has many suspended colloids that take long time to settle. Besides the removal of COD and BOD during waste water treatment, it is necessary to remove the suspended colloidal particles before the final discharge of water into water bodies like lakes, river or ocean. The suspended colloidal particles have a net electrical charge that governs their settling rate. Usually, electrostatic repulsion between the particles makes the suspension highly stable and impedes their settling rate. Hence it becomes necessary to optimize the conditions for flocculation and aggregation of colloidal particles for their efficient removal from the waste water. In order to optimize the flocculation conditions, suspension of kaolin was used to mimic suspended solids of waste water.

The optimization of flocculation with kaolin was studied with purified amyloid protein and three factors viz pH,  $\text{CaCl}_2$  and concentration of amyloid were taken into consideration using CCD (Table. 3.8). The CCD table with varying concentrations of amyloid, pH and  $\text{CaCl}_2$  was generated the experiments were performed at the respective concentration and two responses viz % flocculation and floc size (mm) were recorded after each experiment. The experimental results were obtained the analysis was using the ANOVA analysis. Analysis of, p value of sequential model sum of squares for both flocculation and floc size was less than 0.0001 suggesting quadratic model was appropriate. The variation of data around the fitted model is explained by lack of fit test. The p values for lack of fit tests were insignificant for both % flocculation and floc size, indicating lack of fit for quadratic model was insignificant. The variation in the response predicted by the model is given by the term  $R^2$ . The  $R^2$  values for both flocculation and floc size were greater than 0.9 indicating a satisfactory agreement of the quadratic model to the experimental data.

**Table 3. 8** Optimization of kaolin flocculation by purified amyloid bioflocculant CR4 by central composite design.

Std	Run	Block	Amyloid(mg/l)	CaCl <sub>2</sub> (mg/l)	pH	Flocculation	Floc Size
21	1	Block 1	50.50	0.00	4.50	37.6	1.12
1	2	Block 1	21.07	30.40	3.01	38.7	0.47
27	3	Block 1	50.50	75.00	7.00	10.7	0.07
5	4	Block 1	21.07	119.60	3.01	38.3	0.49
23	5	Block 1	50.50	150.00	4.50	42.7	1.17
8	6	Block 1	79.93	119.60	3.01	81.8	2.59
24	7	Block 1	50.50	150.00	4.50	36.4	1.29
29	8	Block 1	50.50	75.00	4.50	52.8	1.56
19	9	Block 1	100.00	75.0	4.50	51.9	1.54
16	10	Block 1	79.93	119.60	5.99	12.9	0.03
31	11	Block 1	50.50	75.00	4.50	55.3	1.44
28	12	Block 1	50.50	75.00	7.00	17.6	0.08
4	13	Block 1	79.93	30.40	3.01	80.2	2.15
32	14	Block 1	50.50	75.00	4.50	60.1	1.67
3	15	Block 1	79.93	30.40	3.01	85.7	2.58
14	16	Block 1	21.07	119.60	5.99	20.4	0.09
2	17	Block 1	21.07	30.40	3.01	33.0	0.53
17	18	Block 1	1.00	75.00	4.50	0.5	0.05
15	19	Block 1	79.93	119.60	5.99	26.1	0.34
20	20	Block 1	100.00	75.00	4.50	58.9	1.23
11	21	Block 1	79.93	30.40	5.99	22.1	0.09
13	22	Block 1	21.07	119.60	5.99	14.6	0.01
26	23	Block 1	50.50	75.00	2.00	75.5	1.87
6	24	Block 1	21.07	119.60	3.01	42.8	0.53
18	25	Block 1	1.00	75.00	4.50	0.2	0.06
30	26	Block 1	50.50	75.00	4.50	58.2	1.76

Std	Run	Block	Amyloid(mg/l)	CaCl <sub>2</sub> (mg/l)	pH	Flocculation	Floc Size
25	27	Block 1	50.50	75.00	2.00	80.9	2.23
22	28	Block 1	50.50	0.00	4.50	44.9	1.03
10	29	Block 1	21.07	30.40	5.99	20.9	0.10
9	30	Block 1	21.07	30.40	5.99	24.3	0.19
12	31	Block 1	79.93	30.40	5.99	28.8	0.20
7	32	Block 1	79.93	119.60	3.01	87.1	2.50
33	33	Block 1	50.50	75.00	4.50	51.5	1.21
34	34	Block 1	50.50	75.00	4.50	57.8	1.44

**Table 3. 9** ANOVA analysis for optimization of kaolin flocculation by amyloid bioflocculant CR4 using CCD

Source	Sum of Squares	df	Mean Square	F- Value	P- value
Model	19480.49	9	2164.50	88.17	0.0001
A-Amyloid	5200.01	1	5200.01	211.82	0.0001
B-CaCl <sub>2</sub>	8.81	1	8.81	0.36	0.5547
C-pH	10394.33	1	10394.33	423.40	0.0001
AB	3.87	1	3.87	0.16	0.6947
AC	1860.28	1	1860.28	75.78	0.0001
BC	74.43	1	74.43	3.03	0.0945
A <sup>2</sup>	1837.94	1	1837.94	74.87	0.0001
B <sup>2</sup>	478.37	1	478.37	19.49	0.0002
C <sup>2</sup>	147.45	1	147.45	6.01	0.0219
Residual	589.19	24	24.55		
Lack of Fit	236.83	5	47.37	2.55	0.0626

**Table 3. 10** ANOVA analysis of kaolin floc size by CCD.

Source	Sum of Squares	df	Mean Square	F-Value	P-Value
Model	22.98	9	2.55	83.37	0.0001
A-Amyloid	5.74	1	5.74	187.52	0.0001
B-CaCl <sub>2</sub>	0.023	1	0.023	0.76	0.3933
C-pH	11.13	1	11.13	363.44	0.0001
AB	0.022	1	0.022	0.73	0.4017
AC	3.56	1	3.56	116.33	0.0001
BC	0.015	1	0.015	0.49	0.4910
A <sup>2</sup>	2.19	1	2.19	71.57	0.0001
B <sup>2</sup>	0.57	1	0.57	18.60	0.0002
C <sup>2</sup>	0.82	1	0.82	26.70	0.0001
Residual	0.74	24	0.031		
Lack of Fit	0.26	5	0.052	2.08	0.1126

Analysis of variance ANNOVA for flocculation and floc size, shows that, concentration of amyloid and pH had the most significant effect, with p values less than 0.0001. Calcium chloride did not have any significant effect on flocculation activity and floc size. The p value for term AC was less than 0.0001 which indicates significant interaction between amyloid and pH in flocculation and floc size existed (Table. 3.9, Table. 3.10). At central values of CaCl<sub>2</sub> the decrease in pH and increase in amyloid concentration had a significant effect in increasing the flocculating activity and floc size (Figure. 3.6, 3.7). There was also a linear relation between the floc size and the flocculating activity, with a correlation coefficient of 0.95 (Figure. 3.8). This can be explained by the fact that amyloids are linear molecules, and decrease in pH causes protonation of amino groups of protein which imparts net positive charge to the protein molecules. As kaolin particles have net negative charge, the decrease in pH would allow the interaction of amyloid as well as kaolin particles resulting in flocculation. Based on these results the optimum conditions to achieve maximum flocculation activity and floc size was at pH 3 and 72mg/l amyloid concentration.

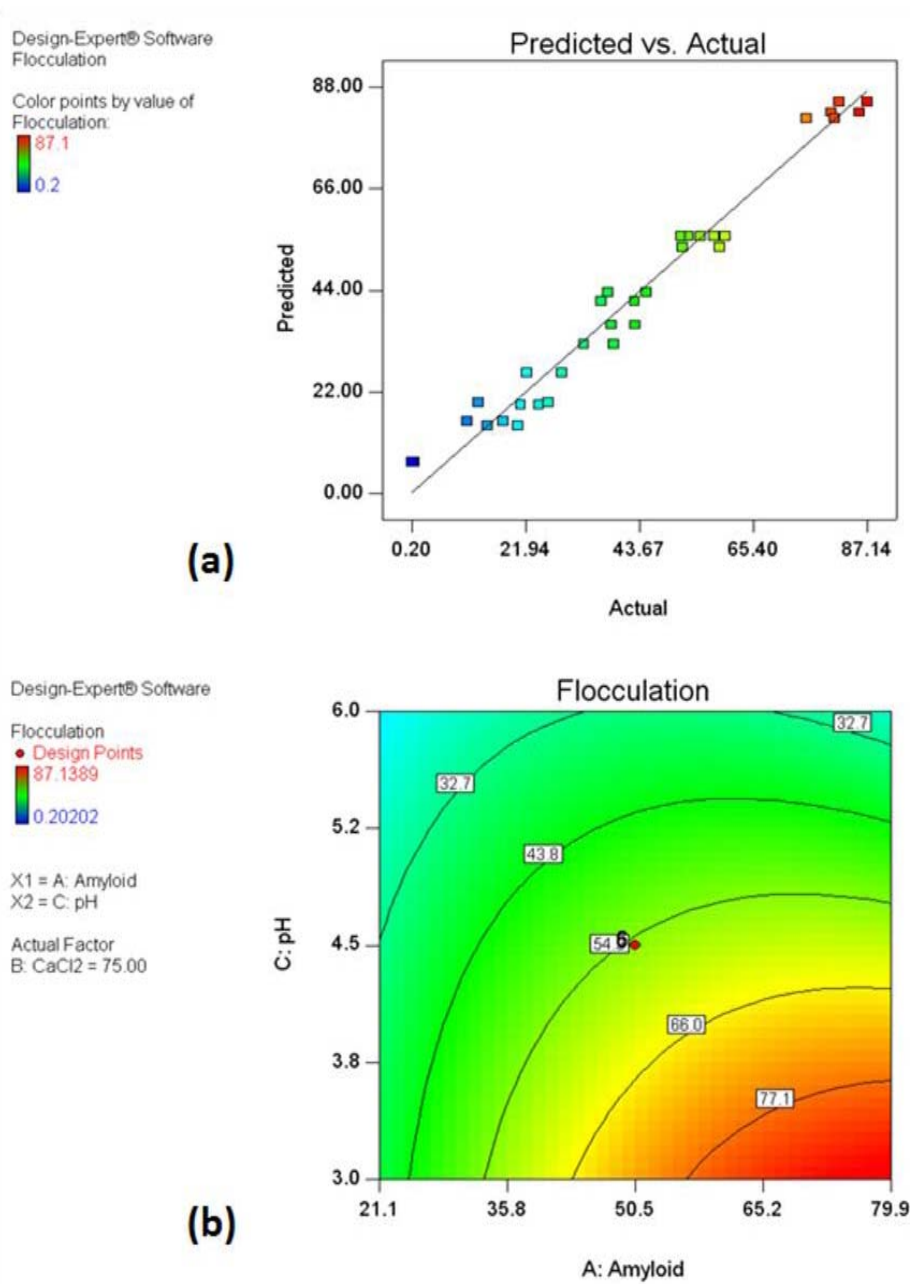


**Figure 3. 6** Optimization of kaolin flocculation by amyloid bioflocculant CR4 using CCD. a) Predicted vs Actual b) Effect of pH and amyloid concentration on flocculation of kaolin

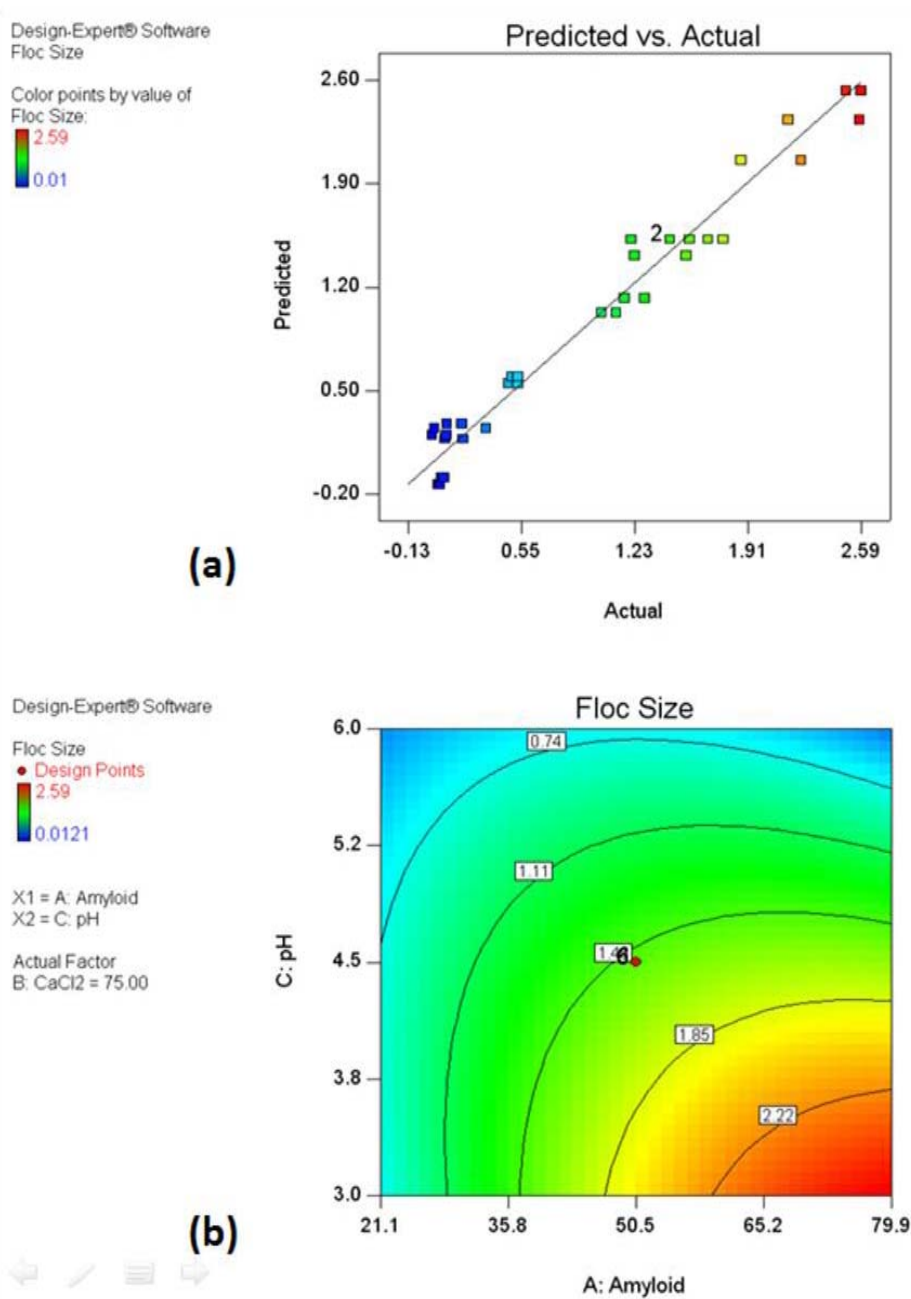


**Figure 3. 7** CCD for optimization of kaolin floc size using CCD. a) Predicted vs Actual b) Effect of pH and amyloid concentration on floc size of kaolin.

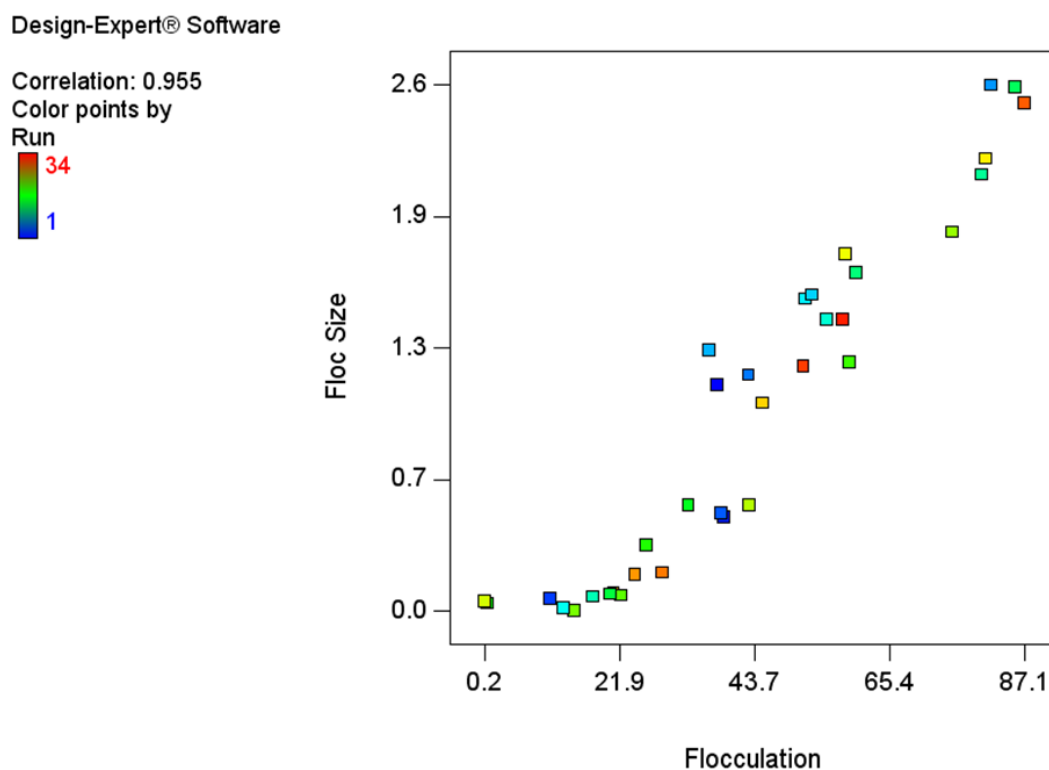


**Figure 3. 8** Correlation between flocculation and floc size during optimization of flocculation of kaolin by amyloid bioflocculant CR4 using central composite design.

### **3.2.3 Scenedesmus cultivation and optimization of its medium**

The recovery of microalgal biomass following cultivation is one of the major rates limiting step for biofuel industries (Vandamme *et al.*, 2013). Majority of the industries working on microalgae employs industrial centrifugation for the biomass harvest. Nevertheless, the operation of such large centrifuges is energy intensive and adds extra cost to the biofuel production. On the other hand, use of bioflocculation can be one of the strategy that can be inexpensive and less energy intensive. Being biodegradable and non toxic in nature the bioflocculants can be used in large amounts without any environmental damage. Hence in order to get efficient and cost-effective method for harvesting of microalgae, flocculation

with amyloid producing bacteria can be an effective way for collecting algal biomass. The flocculation of microalgae was studied with the amyloid producing isolate *B. cereus* CR4. Bacteria and microalgae were grown separately in their respective growth media, and an aliquot of bacterial culture was used as a flocculant for microalgal cells. Addition of *B. cereus* CR4 to the algal culture aggregated the cells indicating its potent application in harvesting of microalgae. Further experiments were carried out to perceive the role of different factors that affects growth of microalgae, flocculation and its optimization.

### **3.2.3.1 Growth of *Scenedesmus* in different media**

Several growth media have been reported for the efficient cultivation of the microalgae. These includes Bold's Basal medium, BG11 medium and Walnes medium. Each medium has its unique composition to support sufficient growth of microalgae. The components of each growth media can also be optimized after screening each component by Plackett Burman analysis followed by response surface methodology.

After the culture of *Scenedesmus* was revived it was subcultured in Bold's basal media for its growth. With an initial optical density (OD 750nm) of 0.007 after inoculation the optical density achieved at the end of 15 days was 0.159 indicating the the growth of microalgae was slow. Once the cell density (OD 750nm) of the culture broth reached at 0.2, different growth media like: Walne's medium and BG11 medium were inoculated with 10% of the culture and analysed for the growth of microalge. The yield of biomass growth was measured as a function of dry weight. Analysis indicated that the average biomass production in Walne's medium was 0.75g/l while that of BG11 medium was 0.64g/l which was several folds high as compared to Bold's basal medium (0.24g/l). Walne's medium showed maximum yield of biomass, with no statically significant difference as compared to BG11 media (Figure. 3.9). This can be explicated by the fact that both BG11 and Walne's media have higher concentration of nitrate and phosphate as compared to Bold's Basal medium. Nitrate and phosphate being essential for microalgal growth produces high yield of biomass. Hence salts of both Walne's and BG11 media were selected for assortment by Plackett Burmann analysis.

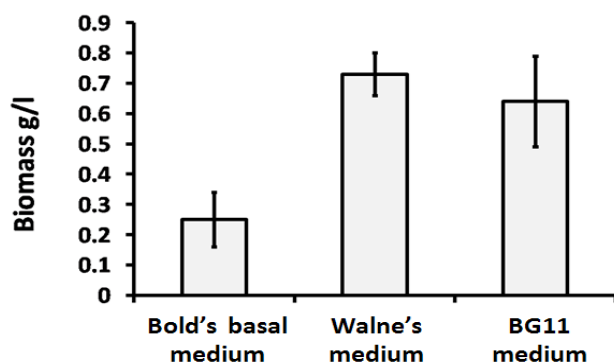


**Figure 3. 9** Growth of *Scenedesmus* sp. in different media

### 3.2.3.2 Plackett Burman analysis of different media components for growth of *Scenedesmus*.

On the basis of biomass production of *Scenedesmus* in different growth media, the salts present in the respective growth media were selected for Plackett Burman analysis. The selected salts encompass:  $\text{NaNO}_3$ ,  $\text{K}_2\text{HPO}_4$ ,  $\text{MgSO}_4$ ,  $\text{CaCl}_2$ ,  $\text{Na}_2\text{CO}_3$ ,  $\text{FeCl}_3$ ,  $\text{ZnSO}_4$ ,  $\text{H}_3\text{BO}_3$  and trace metal elements. The value +1 in the Plackett Burman table indicates the presence of respective salt in the experiment, whereas the value 0 indicates the absence of respective salt (Table. 3.11).

To select the media components that showed significant effect on the growth of algae, F test was performed by taking the ratio of variance due to each factor and the average variance of dummy variable. The critical value for the F-ratio was 2.85, obtained from the statistical table. Any value above 2.85 will show statistically significant effect on growth of microalgae, whereas the value beneath the critical value was considered as statistically insignificant.

**Table 3. 11** Plackett Burmann analysis of different media components for growth of *Scenedesmus*.

Run	NaNO3	K2HPO4	MgSO4	CaCl2	Na2CO3	FeCl3	ZnSO4	H3BO3	Trace metals	Dummy 1	Dummy 2	Biomass yield
1	1	1	0	1	1	1	0	0	0	1	0	<b>225.5</b>
2	0	1	1	0	1	1	1	0	0	0	1	<b>55.88</b>
3	1	0	1	1	0	1	1	1	0	0	0	<b>321.1</b>
4	0	1	0	1	1	0	1	1	1	0	0	<b>194.4</b>
5	0	0	1	0	1	1	0	1	1	1	0	<b>52.11</b>
6	0	0	0	1	0	1	1	0	1	1	1	<b>216.7</b>
7	1	0	0	0	1	0	1	1	0	1	1	<b>355.8</b>
8	1	1	0	0	0	1	0	1	1	0	1	<b>237.1</b>
9	1	1	1	0	0	0	1	0	1	1	0	<b>327.8</b>
10	0	1	1	1	0	0	0	1	0	1	1	<b>72.15</b>
11	1	0	1	1	1	0	0	0	1	0	1	<b>166.1</b>
12	0	0	0	0	0	0	0	0	0	0	0	<b>13.66</b>

**Table 3. 12** F test for Plackett Burman analysis of the optimization of media for growth of *Scenedesmus* sp.

Factor	Variance	F Value
<b>NaNO3</b>	88151.02	30.44
<b>K2HPO4</b>	13.31	0.00
<b>MgSO4</b>	5126.16	1.77
<b>CaCl2</b>	1966.08	0.68
<b>Na2CO3</b>	1603.60	0.55
<b>FeCl3</b>	38.59	0.01
<b>ZnSO4</b>	41425.80	14.30
<b>H3BO3</b>	4294.84	1.48
<b>Trace metals</b>	1878.0	0.65
<b>Dummy 1</b>	5712.47	
<b>Dummy 2</b>	79.25	

In this case, NaNO<sub>3</sub> and ZnSO<sub>4</sub> showed the F-value of 30.44 and 14.3 respectively (Table. 3.12). This indicates that both NaNO<sub>3</sub> and ZnSO<sub>4</sub> had a significant contribution in the growth

of *Scenedesmus*. Hence based on these results, NaNO<sub>3</sub> and ZnSO<sub>4</sub> were selected for optimization of growth of *Scenedesmus* by response surface methodology.

### 3.2.3.3 Response surface methodology for media optimization (CCD)

As described earlier the response surface methodology by central composite design is one of the efficient methods for achieving desired optimum results. The salts demonstrating significant effect on growth were selected by Plackett Burmann analysis. Two salts viz NaNO<sub>3</sub> and ZnSO<sub>4</sub> had significant effect in supporting the growth of *Scenedesmus*. Both NaNO<sub>3</sub> and ZnSO<sub>4</sub> were selected for optimization by CCD of response surface methodology. Different range of NaNO<sub>3</sub> and ZnSO<sub>4</sub> were selected and generation of CCD table (Table. 3.13) was done by design expert software (Version 9.0). The minimum concentration of NaNO<sub>3</sub> was fixed at 2 mg% while the maximum was fixed at 200 mg%. In case of ZnSO<sub>4</sub> the maximum concentration was fixed at 5 mg% while minimum was fixed at 0.05 mg%. The response of the CCD was documented as dry weight of biomass, measured after cultivation (Table. 3.13). The ANOVA analysis for CCD is depicted in table 3.14.

**Table 3. 13** Central composite design for the optimization of NaNO<sub>3</sub> and ZnSO<sub>4</sub> concentrations for the % growth of *Scenedesmus*

Std	Run	Block	A: NaNO <sub>3</sub> (mg%)	B: ZnSO <sub>4</sub> (mg%)	Biomass (g/l)
1	1	Block 1	31.00	0.77	0.066
9	2	Block 1	101.00	2.52	2.3
3	3	Block 1	31.00	4.28	0.467
7	4	Block 1	101.00	0.05	0.365
6	5	Block 1	200.00	2.52	1.44
8	6	Block 1	101.00	5.00	0.85
5	7	Block 1	2.00	2.52	0.359
4	8	Block 1	171.00	4.28	1.82
2	9	Block 1	171.00	0.77	0.676

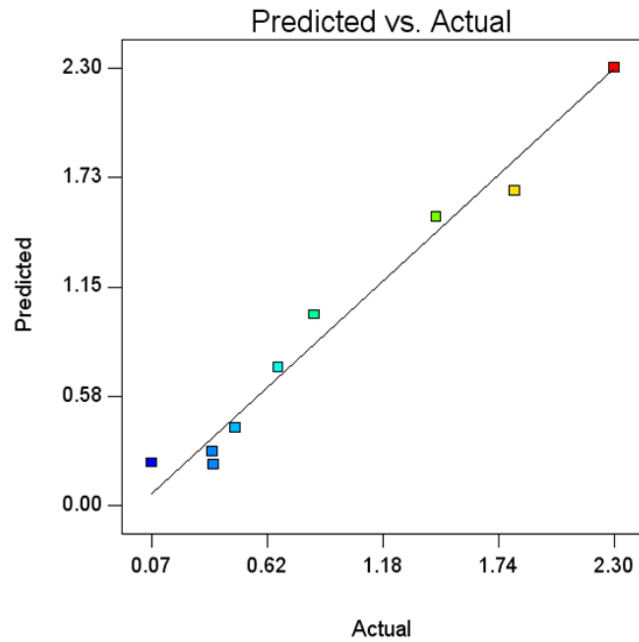
**Table 3. 14 ANOVA analysis for the medium optimization for cultivation of *Scenedesmus*.**

Source	Sum of Squares	df	Mean Square	F-Value	p-Value
Model	4.49	5	0.90	23.25	0.0132
A-NaNO <sub>3</sub>	1.52	1	1.52	39.46	0.081
B-ZnSO <sub>4</sub>	0.62	1	0.62	16.11	0.0278
AB	0.14	1	0.14	3.57	0.1551
A <sup>2</sup>	1.42	1	1.42	36.84	0.0090
B <sup>2</sup>	2.08	1	2.08	53.83	0.0052
Residual	0.12	3	0.039		

The figure 3.10 depicts the contour plots for the optimal growth of *Scenedesmus*. At 125mg% of NaNO<sub>3</sub> and 2.55mg% of ZnSO<sub>4</sub> about 3.46g/l of biomass yield was speculated. The predicted value of biomass yield was confirmed experimentally at the respective concentrations of NaNO<sub>3</sub> and ZnSO<sub>4</sub>. The experimental yield so obtained was 3.16g/l which was statistically analogous with respect to the predicted value. In case of *Scenedesmus* it has been documented that nitrogen sources like urea, Ammonium chloride, Sodium nitrate, Potassium nitrate, Calcium nitrate supports good growth. Out of all Potassium nitrate and Sodium nitrate are one of the most preferred nitrogen source that supports growth and biomass production (Arumugam *et al.*, 2013). A recent study on microalgae by Podevin *et al.*, (2015) elaborates that most of the microalgae like *C. vulgaris*, *N. oculata* and *C. Sorokiniana* demonstrates maximum biomass yield when grown in presence of sodium nitrate as a nitrogen source.

Design-Expert® Software  
Biomass

Color points by value of  
Biomass:  
2.3  
0.066



Design-Expert® Software

Biomass  
● Design Points  
2.3  
0.066

X1 = A: NaNO<sub>3</sub>  
X2 = B: ZnSO<sub>4</sub>

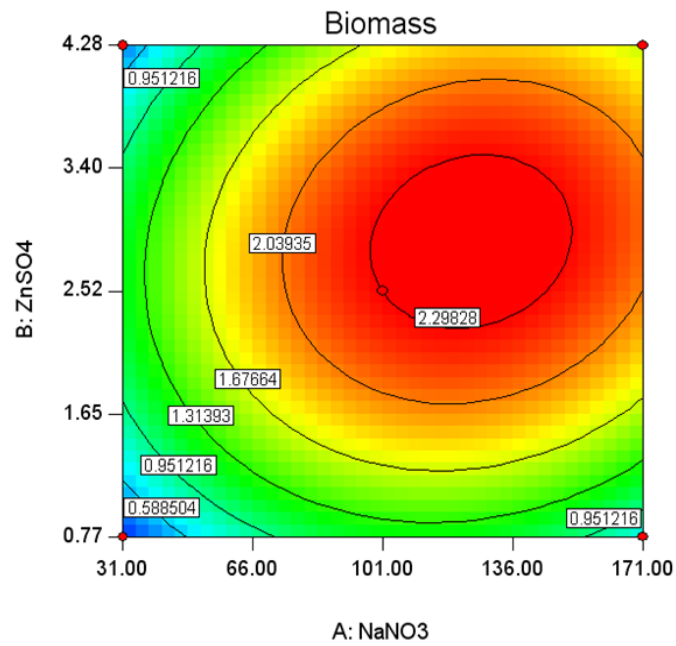


**Figure 3. 10** CCD for optimization of NaNO<sub>3</sub> and ZnSO<sub>4</sub> for the growth of *Scenedesmus*  
a) Predicted vs Actual. b) Effect of NaNO<sub>3</sub> and ZnSO<sub>4</sub> concentration on biomass production of *Scenedesmus*

### 3.2.3.4 Optimization of flocculation of microalgae by Response surface methodology

Preliminary studies with the flocculation of *Scenedesmus* sp. cells shows that influence of  $Fe^{+3}$  was marked out of many metal ions like calcium chloride, copper sulphate, sodium chloride, ferric chloride, potassium chloride, manganese chloride, and magnesium chloride were tested (Figure. 3.11). The conditions for flocculation of microalgae was optimized by central composite design. Table 3.15 indicates the effect of  $Fe^{+3}$ , pH and cell density on flocculation and floc size of *Scenedesmus* sp.

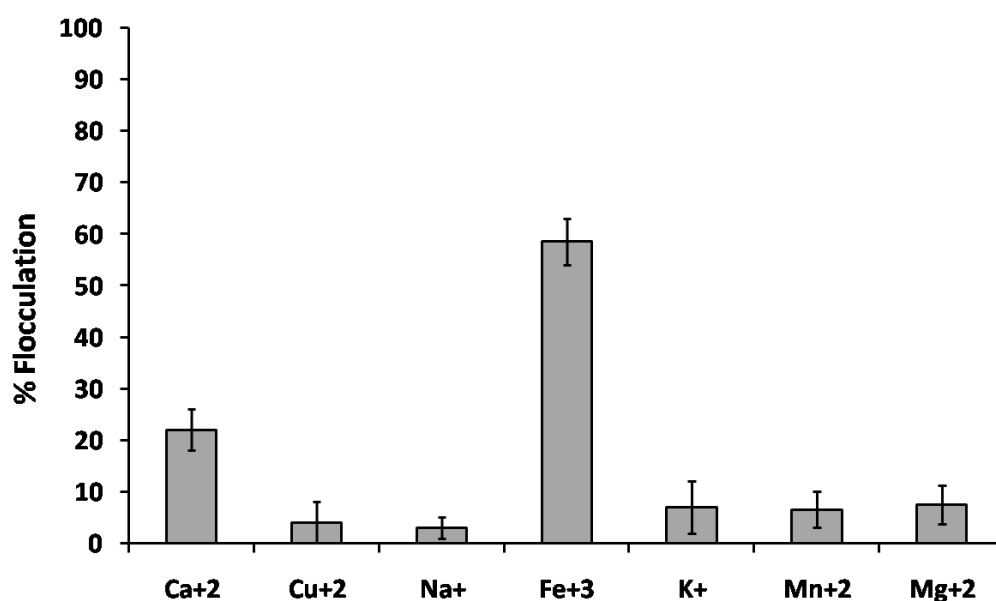


**Figure 3. 11** Effect of metal ions on flocculation of *Scenedesmus* by *B.cereus* CR4.

The results documented in Table 3.15 indicates that maximum 82.3% flocculation and 1.9mm average floc size can be obtained when the pH, biomass and  $Fe^{+3}$  concentration are adjusted to 4.0, 0.400 (OD 750nm) and 187 mg% respectively. The ANOVA table for the quadratic equation for the prediction of % flocculation and floc size are described in Table 3.16 and Table 3.17 respectively. Both the tables show p-value for the model less than 0.0001 which indicates that the mathematical equation generated for the prediction of response at different concentration of pH, biomass and  $Fe^{+3}$  ions was accurate.

**Table 3. 15** Design of experiment and analysis for optimization of *Scenedesmus* sp. flocculation by *B. cereus* CR4 using CCD

std	Run	Block	Fe	pH	Biomass	Flocculation	Flocsize
11	1	Block 1	125.00	3.00	0.80	75.1	1.6
1	2	Block 1	62.50	4.00	0.40	25.3	0.0
4	3	Block 1	187.50	6.00	0.40	60.1	1.2
9	4	Block 1	0.00	5.00	0.80	12.3	0.0
14	5	Block 1	125.00	5.00	1.60	72.1	1.3
3	6	Block 1	62.50	6.00	0.40	32.2	0.1
13	7	Block 1	125.00	5.00	0.00	33.6	0.1
2	8	Block 1	187.50	4.00	0.40	82.3	1.9
15	9	Block 1	125.00	5.00	0.80	78.2	1.5
6	10	Block 1	187.50	4.00	1.20	82.2	1.9
16	11	Block 1	125.00	5.00	0.80	77.6	1.6
12	12	Block 1	125.00	7.00	0.80	67.1	1.2
5	13	Block 1	62.50	4.00	1.20	65.5	1.4
7	14	Block 1	62.50	6.00	1.20	70.2	1.7
8	15	Block 1	187.50	6.00	1.20	80.1	1.7
10	16	Block 1	250.00	5.00	0.80	67.7	1.2

The mathematical equation was further validated by analysis of p-value for lack of fit test in the ANOVA table. The lack of fit test for % flocculation and floc size were 0.07 and 0.133 respectively indicating that the lack of fit test was insignificant. The final confirmation for the equation was done by analyzing the graph of predicted vs actual (Figure. 3.12). The predicted response with the use of mathematical equation have been demonstrated in the respective contour plots (Figure. 3.13). The results indicate that acidic pH and increase in concentration of  $Fe^{+3}$  along with increase in cell density of *B. cereus* CR4 favours flocculation of microalgae. Very low flocculation was obtained when pH was kept at neutral and  $Fe^{+3}$  concentration was low. The optimized results are demonstrated in (Figure. 3.13).

**Table 3. 16** ANOVA analysis for Optimization of *Scenedesmus* sp. flocculation by *B. cereus* CR4 using CCD

Source	Sum of Squares	df	Mean Square	F-Value	p-Value
Model	7470.10	9	830.01	48.13	0.0001
A-Fe <sup>+3</sup>	3088.58	1	3088.58	179.08	0.0001
B-pH	51.48	1	51.48	2.98	0.1348
C-Biomass	1916.25	1	1916.25	111.11	0.0001
AB	161.10	1	161.10	9.34	0.0223
AC	424.86	1	424.86	24.63	0.0025
BC	40.05	1	40.05	2.32	0.1784
A <sup>2</sup>	1436.41	1	1436.41	83.29	0.0001
B <sup>2</sup>	46.24	1	46.24	2.68	0.1527
C <sup>2</sup>	627.50	1	627.50	36.38	0.0009
Residual	103.48	6	17.25		
Lack of Fit	103.30	5	20.66	114.78	0.0707

The predicted results show that optimum flocculation can be obtained at 182mg/l Fe<sup>+3</sup> concentration, pH 4 and bioflocculant cell density of 1.1 (OD 600nm). The predicted values were confirmed experimentally where enhanced flocculation of 85.4% was achieved which was statistically similar when compared with the predicted value. There was also a strong correlation between % flocculation of *Scenedesmus* and its floc size (Figure. 3.16). The results demonstrate the role of pH, concentration of Fe<sup>+3</sup> and cell density on floc size of microalgae. The floc size was 1.9mm large when the pH was 4, 182mg/l Fe<sup>+3</sup> and cell density of 1.1(OD 600nm).

**Table 3. 17** ANOVA analysis for optimization of *Scenedesmus* floc size by CCD

Source	Sum of Squares	df	Mean Square	F-Value	p-Value
Model (Floc size)	6.77	9	0.75	15.54	0.0017
A-Fe <sup>+3</sup>	2.23	1	2.23	46.03	0.0005
B-pH	0.091	1	0.091	1.88	0.2191
C-Biomass	2.21	1	2.21	45.64	0.0005
AB	0.16	1	0.16	3.32	0.1184
AC	0.71	1	0.71	14.58	0.0088
BC	0.074	1	0.074	1.52	0.2637
A <sup>2</sup>	0.83	1	0.83	17.06	0.0061
B <sup>2</sup>	0.026	1	0.026	0.53	0.4943
C <sup>2</sup>	0.72	1	0.72	14.83	0.0084
Residual	0.29	6	0.048		
Lack of Fit	0.29	5	0.058	32.05	0.1333

Figure 3.17 shows the flocculation of microalgae under optimized conditions. The experimental flask shows aggregated cells of *Scenedesmus* sp. In presence of amyloid producing *B. cereus* CR4, under optimized conditions. The control flask was set up with no bioflocculant added (Figure. 3.17a). The samples from each flask were taken on the glass slide and studied under bright field microscope. Whereas the sample from the control flask showed free algal cells that were not aggregated. Figure. 3.17b, dense aggregated flocs of microalgal cells were observed when the flocculation was carried out under optimized conditions (Figure. 3.17c).

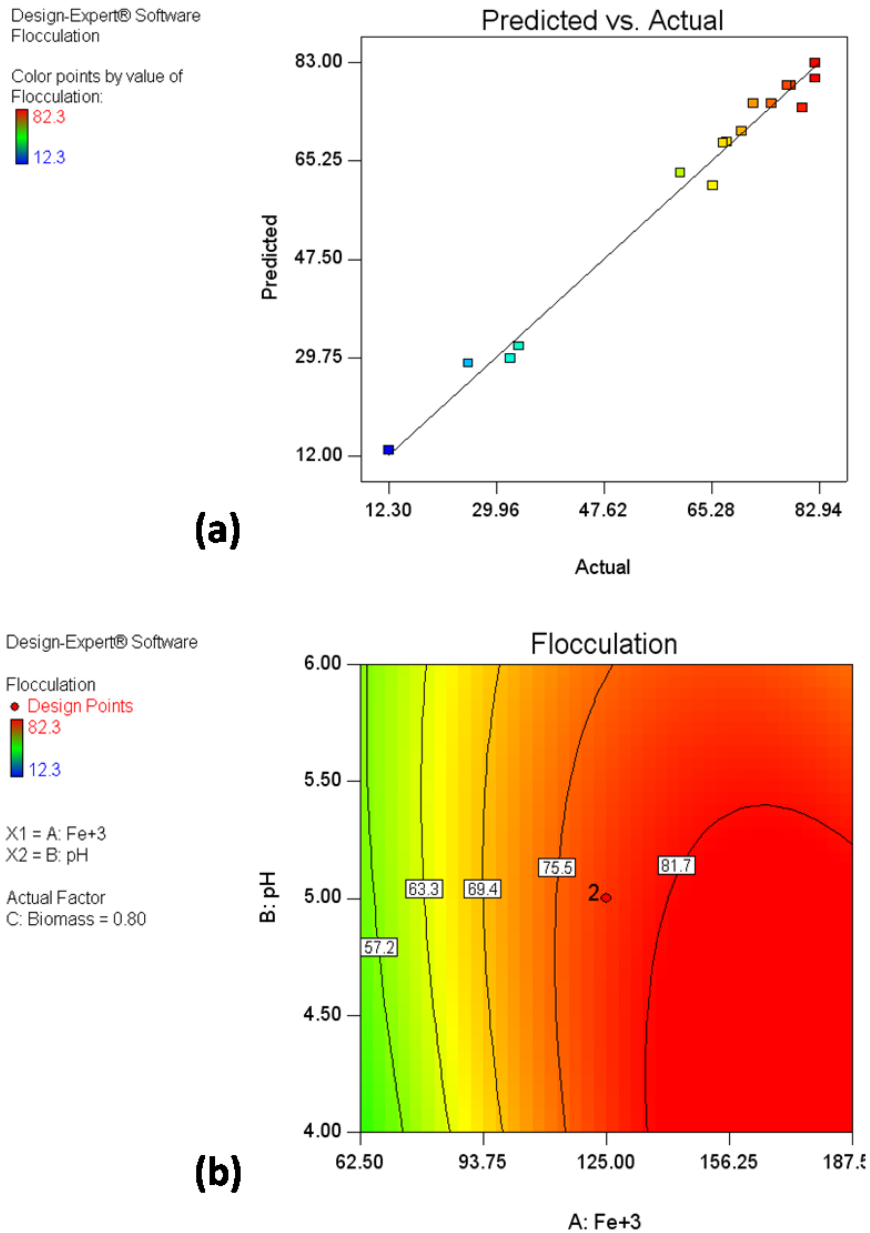


**Figure 3. 12** Contour plots for optimization of pH and Fe<sup>+3</sup> required for flocculation of *Scenedesmus* sp. by *B. cereus* CR4 a) Predicted vs Actual b) Effect of pH and Fe<sup>+3</sup> on flocculation of *Scenedesmus*

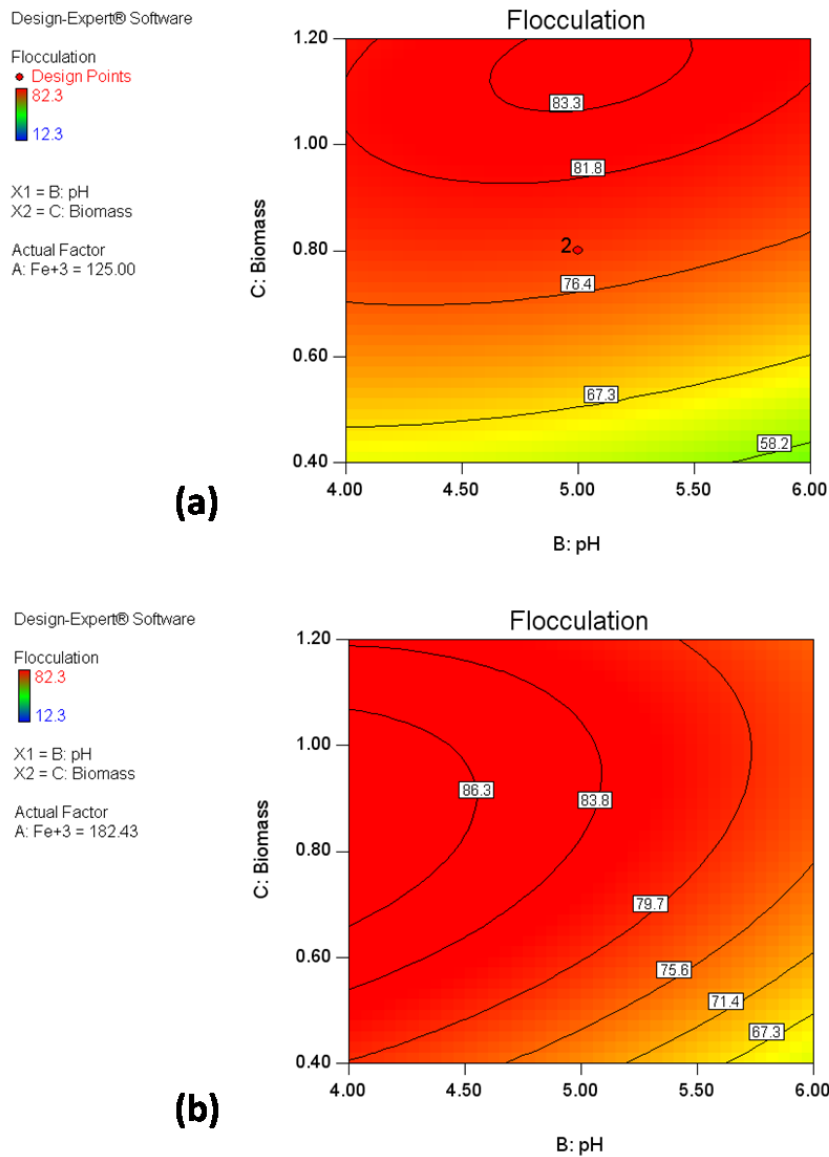


**Figure 3. 13** Contour plots for optimization of biomass, pH and Fe<sup>+3</sup> required for flocculation of *Scenedesmus* sp. by *B. cereus* CR4 a) Effect of biomass and pH at 125 mg% of Fe<sup>+3</sup> on flocculation of *Scenedesmus* b) Effect of biomass and pH at 182 mg% of Fe<sup>+3</sup> on flocculation of *Scenedesmus*.

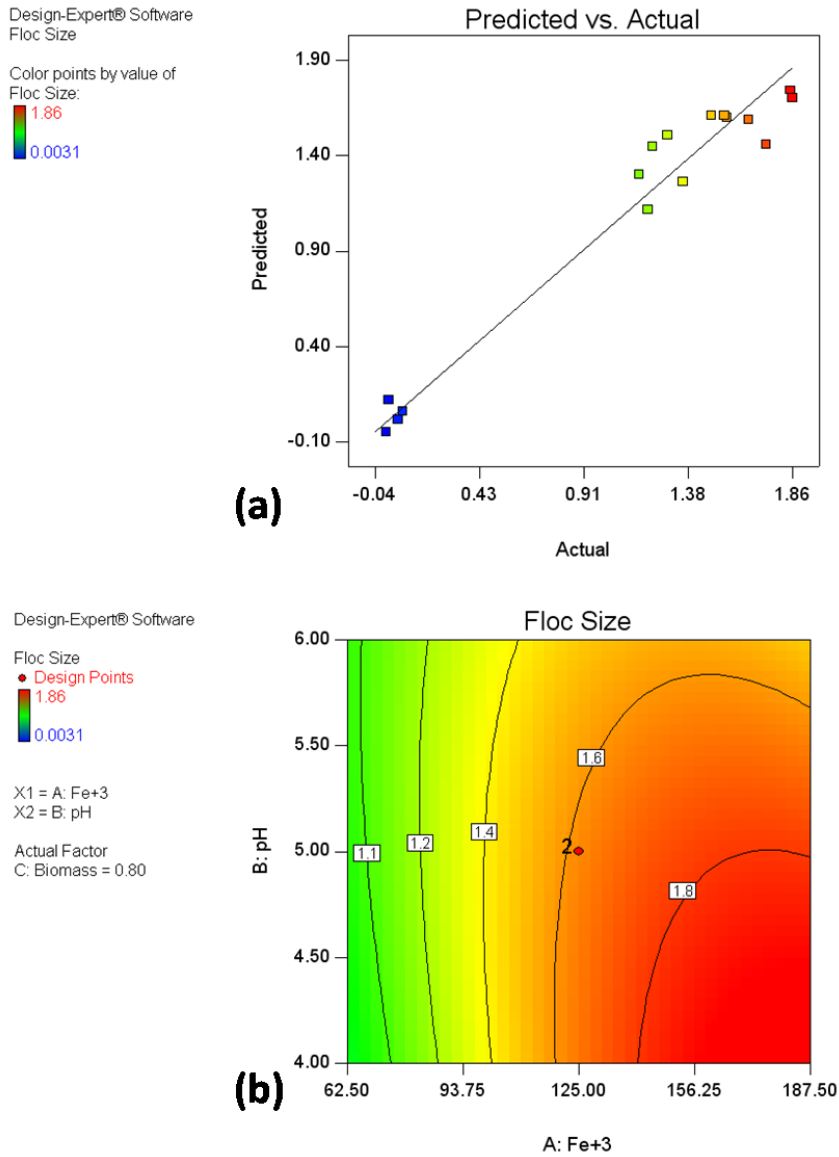


**Figure 3. 14** Contour plots for optimization of pH and  $\text{Fe}^{+3}$  on floc size after flocculation of *Scenedesmus* sp. by *B. cereus* CR4 a) Predicted vs Actual b) Effect of pH and  $\text{Fe}^{+3}$  on floc size of *Scenedesmus* sp.

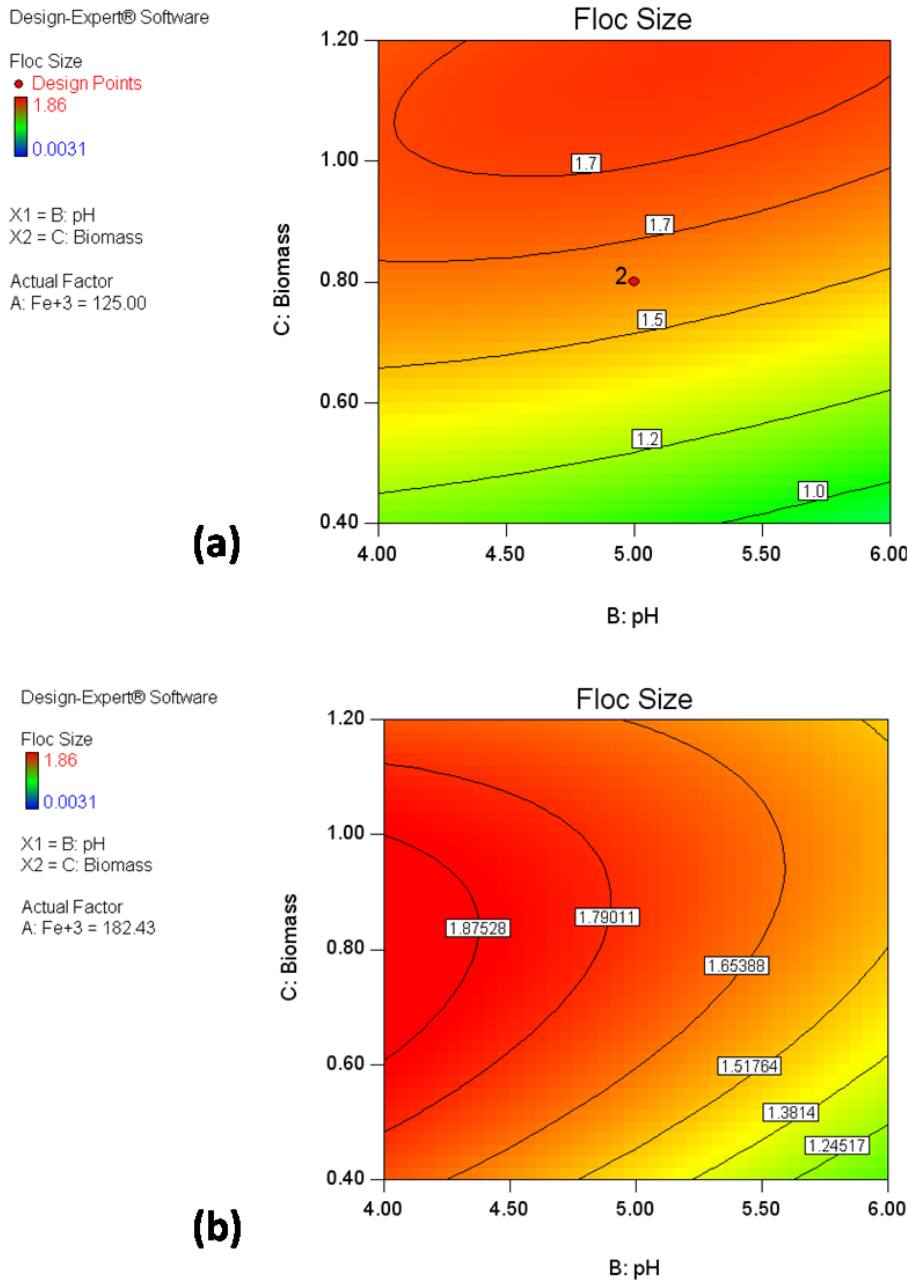


**Figure 3. 15** Contour plots showing effect of pH, Fe<sup>+3</sup> and cell density (biomass) on floc size of *Scenedesmus*

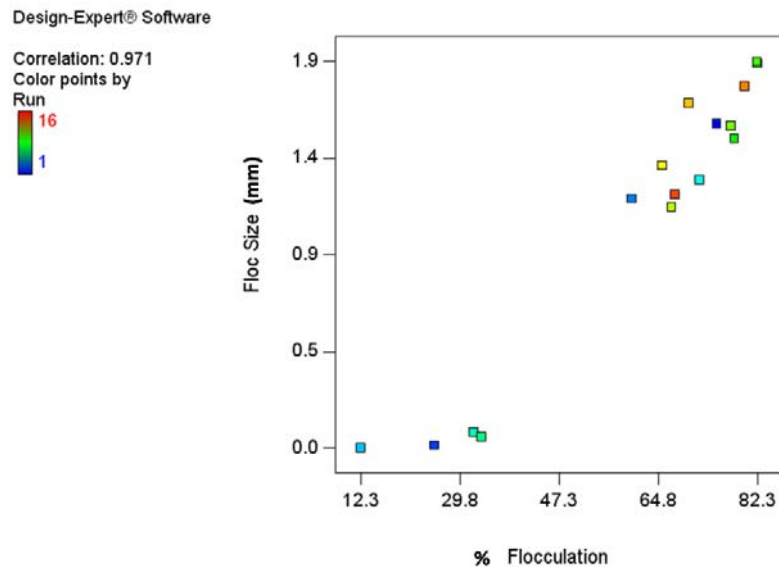


**Figure 3. 16** Correlation between % flocculation and floc size of *Scenedesmus* sp.

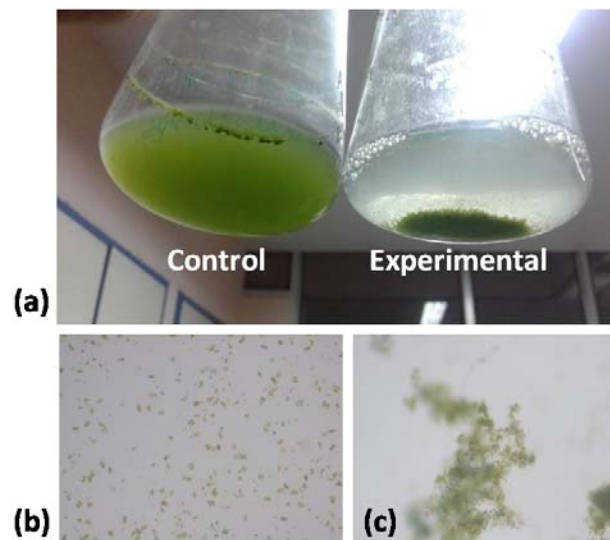


**Figure 3. 17** Flocculation of *Scenedesmus* using *B. cereus* CR4 under optimized conditions. a) Suspended biomass of *Scenedesmus* in absence of *B. cereus* CR4 (control). Aggregated biomass of *Scenedesmus* in presence of *B. cereus* CR4 (experimental). b) Bright field microscopy of *Scenedesmus* in absence of bioflocculant CR4. c) Bright field microscopy of flocs of *Scenedesmus* sp.

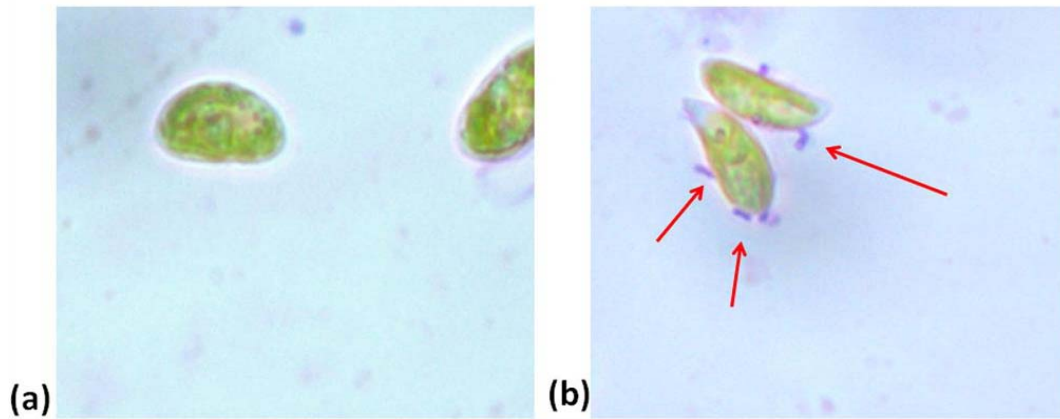


**Figure 3. 18** Interaction of *B.cereus* CR4 cells with *Scenedesmus* cells. a) *Scenedesmus* sp. cells in absence of *B. cereus* CR4 b) *Scenedesmus* sp. cells in presence of *B.cereus* CR4

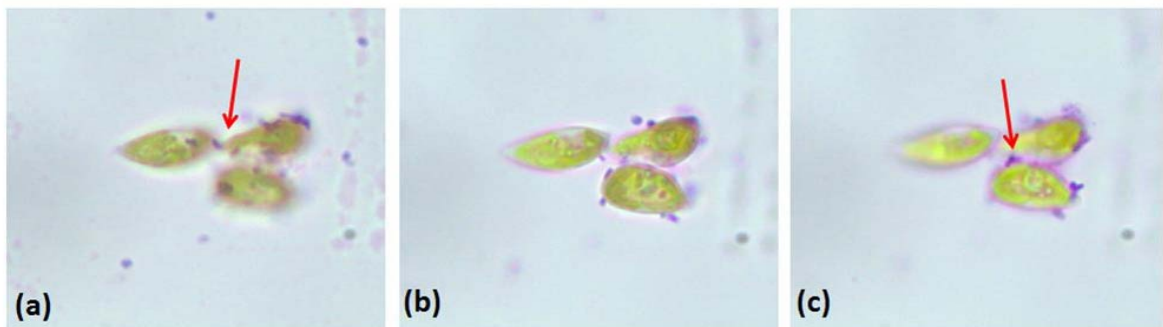


**Figure 3. 19** Role of *B.cereus* CR4 in flocculation of *Scenedesmus* showing patching mechanism. (a), (b) and (c) demonstrates images of different focal plane of microalgal flocs studied under bright field microscope.

Bioflocculants are known to cause aggregation of particles either by the formation of bridge around the particles or by patching mechanism. This phenomenon is widely studied using transmission or scanning electron microscope where the biopolymer interacting with the particles can be easily visualized. However, the microalgal cells being large in size can be easily visualized under the bright field microscope. Hence to investigate the mechanism by which *B. cereus* CR4 aggregates *Scenedesmus* sp. cells, the cells of *B. cereus* CR4 were

prestained with crystal violet and used for flocculation. Untreated microalgal biomass was used as a control (Figure. 3.17b). The aggregated microalgal biomass was collected and examined under bright field microscope with 450X magnification (Figure. 3.17c). Microscopic study reveals that under optimized conditions the bacterial cells easily attach themselves on the surface of microalgal cells (Figure. 3.18b).

Further investigations (Figure. 3.19) was carried out by observing the same floccules of microalgae under different focal plane. Analysis of the microalgal floccules demonstrates the role of bacterial cells in aggregation of microalgal cells by patching mechanism (Figure. 3.19 c) indicated by red arrow. By taking dimensions of bacterial cell and algal cell into consideration, the size of bacterial cells is negligible as compared to the microalgal cells and small size of single bacterium may not be able to hold large sized microalgal cells. However, the use of  $\text{Fe}^{+3}$  ions as a coagulant neutralizes surface charge of microalgal cells allowing them to come together. This coagulation is followed by flocculation by patch formation after addition of bacterial cells. Thus, the patch mechanism for flocculation of *Scenedesmus* sp. was confirmed.

### **3.2.4 Factors affecting cell viability of *Scenedesmus* sp.**

#### **3.2.4.1 Effect of pH and $\text{Fe}^{+3}$ on cell viability and growth**

Once the conditions for flocculation of *Scenedesmus* sp. with *B. cereus* CR4 was optimized the next strategy was to co-cultivate *B. cereus* CR4 and *Scenedesmus* sp. together and optimize the conditions for aggregated growth of the microalgae. The co-cultivation strategy can be highly beneficial as it can eliminate the huge cost of harvesting.

Careful observation of the aggregated cells demonstrated that the flocculated algal biomass turns yellow within 24hrs after flocculation while the free suspension of the microalgal cells remain green. Thus, flocculation of microalgal cells was found to be cytotoxic as indicated by the chlorosis of microalgal biomass. On the basis of this observation, it was hypothesized that either pH or  $\text{Fe}^{+3}$  ions, may be toxic for the microalgal cells. Hence experiments were carried out to study the effect of pH and  $\text{Fe}^{+3}$  concentration on algal cell viability, growth and

flocculation. The role of bacterial cells in chlorosis of microalgal biomass was ruled out as most of previous studies have demonstrated mutualistic role of microalgae and bacteria in supporting each others growth (Ravindran *et al.*, 2016). On the other hand, drastic change in pH and presence of metal ions can significantly alter the viability and growth of microalgal cells. Metals such as Fe, Cu, and Zn play an important role as cofactors of the enzymes involved in photosynthesis (Volland *et al.*, 2014). However, excess of any metal ions can lead to oligodynamic action which can prove lethal for algal cells.

Hence to check whether the chlorosis of microalgal biomass after flocculation was due to acidic pH or  $\text{Fe}^{+3}$  ions, response surface methodology was used. With the aid of Design expert software, using central composite design the microalgal cell viability and growth was measured at various concentration of  $\text{Fe}^{+3}$  ions and pH. The measurement of the cell viability was done by bright field microscopy, after staining the cells with methylene blue. The dead cells emerge blue while the live cells appeared green in color (Figure. 3.20). The response in terms of the microscopic cell counts for the central composite design are depicted in Table 3.18. The table demonstrates that average maximum cell viability of 92.8% was accounted at 0.55mg%  $\text{Fe}^{+3}$  ions and pH 6, while the cell viability was dropped to 8% when the pH was set at 2. Table 3.18 shows the results of central composite design in terms of % viability and growth.

Analysis of the CCD results showed that the linear regression model was followed in predicting the experimental response. Based on linear regression model the graphs for growth and % cell viability were plotted as a function of pH and concentration of  $\text{Fe}^{+3}$  ions (Figure. 3.21 and 3.22)

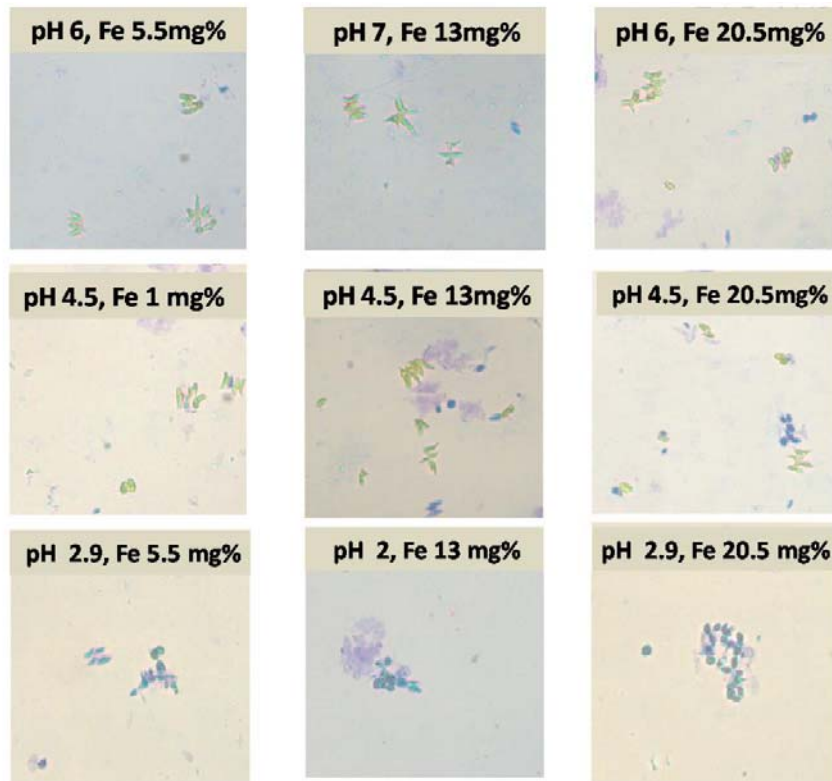


**Figure 3. 20** Effect of  $Fe^{+3}$  and pH on cell viability of *Scenedesmus* sp.

**Table 3. 18** Optimization of Factors affecting cell viability of *Scenedesmus* sp. by CCD.

std	Run	Block	pH	Fe(mg%)	% Flocculation	growth(g/l)	Viability %
6	1	Block 1	7.0	13.00	32.9	2.0	90.8
1	2	Block 1	3.0	5.50	62.776	0.1	11.9
4	3	Block 1	6.0	20.50	45.47	1.4	84.7
7	4	Block 1	4.5	1.00	25.59	0.1	8.8
8	5	Block 1	4.5	25.00	54.19	0.2	56.8
5	6	Block 1	2.0	13.00	63.95	0.1	34
3	7	Block 1	3.0	20.50	71.78	0.1	10.4
9	8	Block 1	4.5	13.00	50.17	0.2	53.9
2	9	Block 1	6.0	5.50	17.01	1.5	95.2

Figure 3.21a demonstrates growth of *Scenedesmus* at different pH. Analysis shows that an increase in  $\text{Fe}^{+3}$  concentration from 5.5 to 20.5 mg% did not have any negative effect on viability of *Scenedesmus sp.* while change in pH from 6 to pH 3 had a drastic effect. At neutral pH about 99% of the cells were viable. When the pH value dropped upto 4.5 about 50.4% of the cells were viable while at pH 3 and below the cell viability was negligible was decreased by 91.2% (Figure. 3.21b). These results stipulate that there was no negative role of  $\text{Fe}^{+3}$  ions on cell viability. Indeed, the cell viability of *Scenedesmus sp.* was improved by 22.5% when the concentration of  $\text{Fe}^{+3}$  was increased from 5.5 to 20.5 mg% at pH 3 (Figure. 3.22a). These results conclude that pH below 4.5 was lethal for microalgal cells (Figure. 3.22b) .

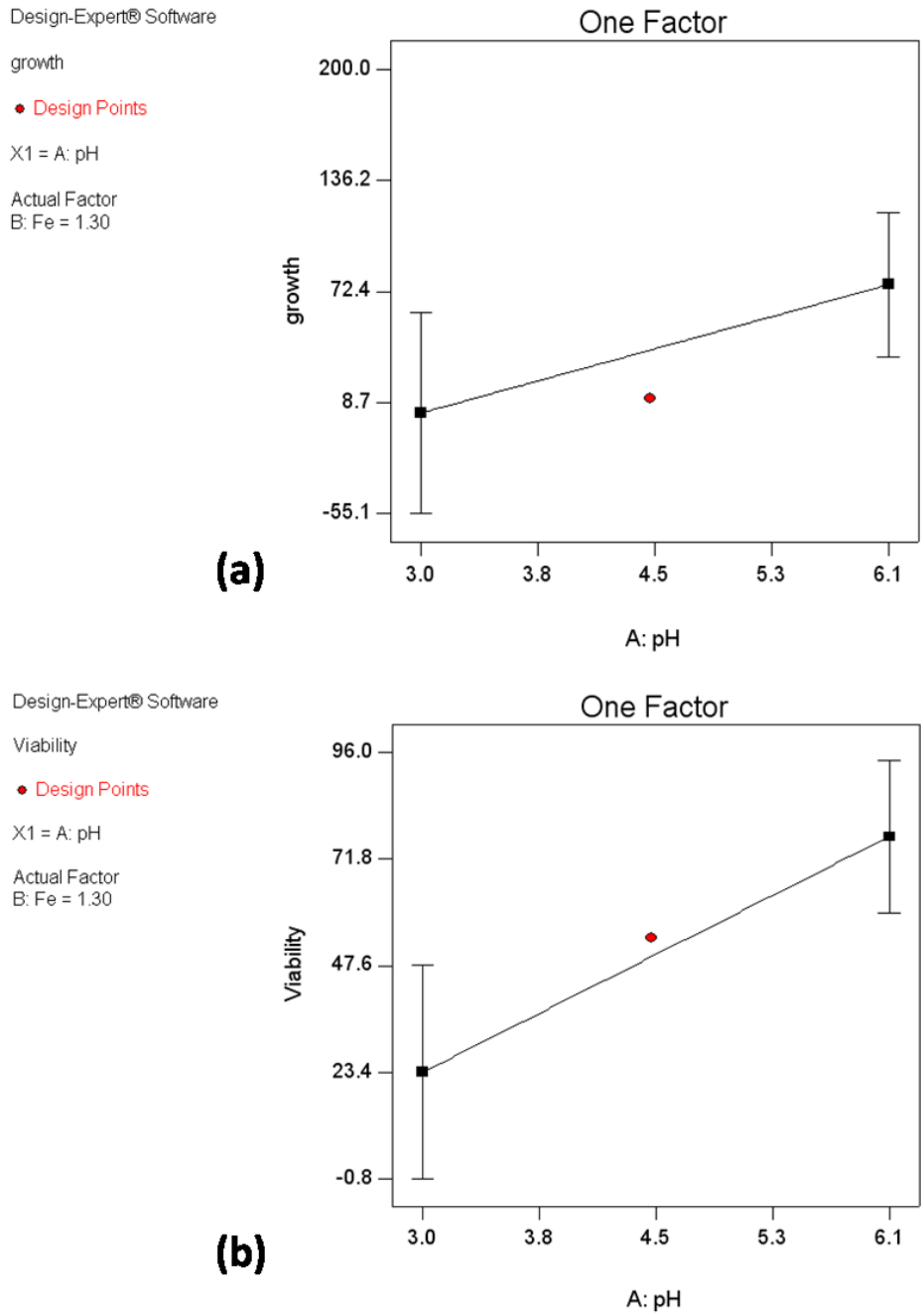


Figure 3. 21 Effect of pH on cell viability and growth of *Scenedesmus* sp..

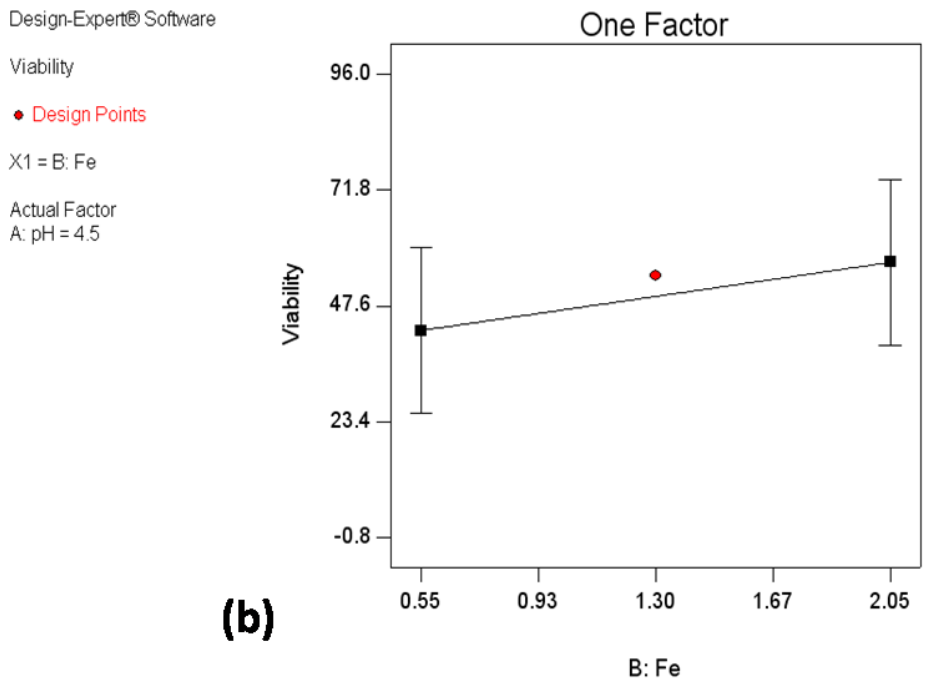
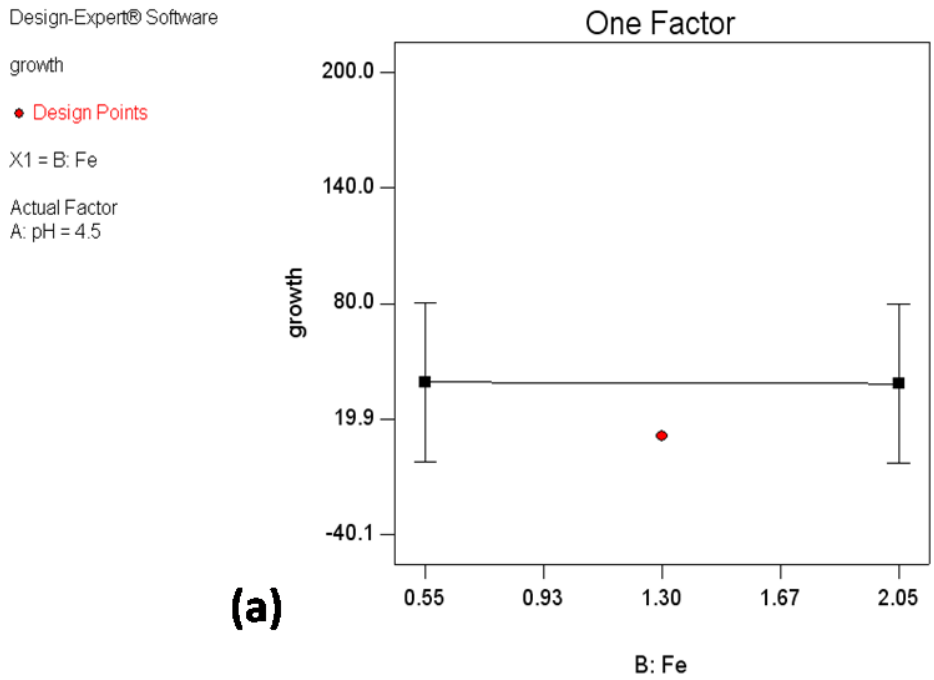


Figure 3. 22 Effect of  $Fe^{+3}$  on cell viability and growth of *Scenedesmus* sp.

#### **3.2.4.2 Effect of microalgal growth media on growth and bioflocculant CR4 production by *B. cereus* CR4**

Once the factors affecting microalgal growth and viability were studied, the next step involved the study of algal growth media on biomass and bioflocculant production by *B. cereus* CR4. This study was important as the bacteria requires nutrient rich medium for its growth and bioflocculant production while the microalgal cells requires media with only minimal salts.

Preliminary experiments showed that bacterial growth was abrogated in the algal media devoid of carbon source whereas the algal media fortified with glucose and lactose did show significant increase in growth (Figure. 3.23). However, the flocculation activity associated with the bacterial biomass was reduced by several fold in the minimal media (Figure. 3.24). Hence in order to augment flocculation by bacterial cells, it was hypothesized that increase in bacterial cell density may improve the flocculation activity. Hence to test this hypothesis, flocculation was checked with different cell density of *B. cereus* CR4 cultivated in the different minimal medium. Flocculation studies at higher cell density braced the hypothesis and showed increased flocculation. The increase in cell density from 0.1 OD (600nm) to 0.7 OD increased the flocculation activity from 15.3% to 70% (Figure. 3.25). Keeping these observations in mind, further optimization studies were carried out to maintain bacterial cell density as well as algal growth to optimum, for efficient aggregated growth during cocultivation.

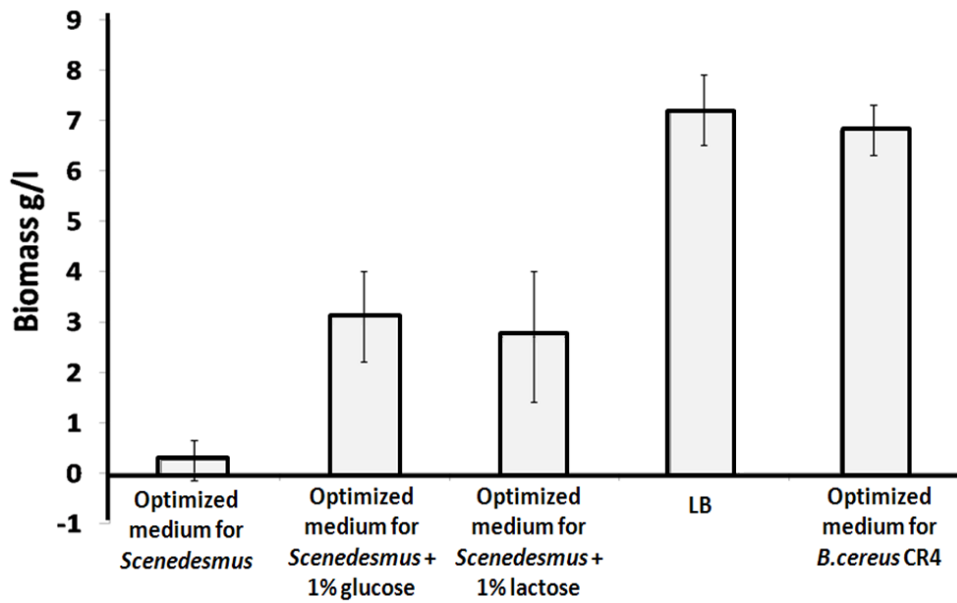


Figure 3. 23 Growth of *B. cereus* CR4 in different media.

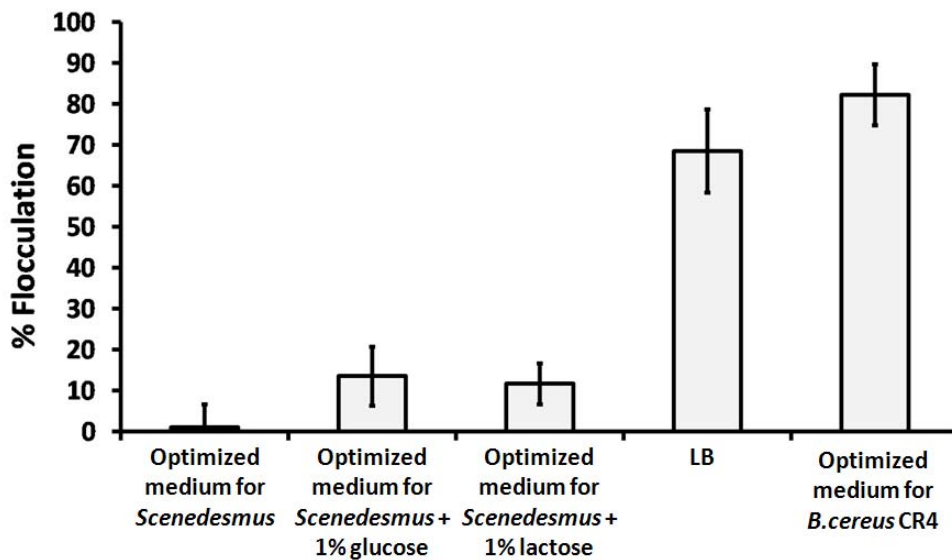
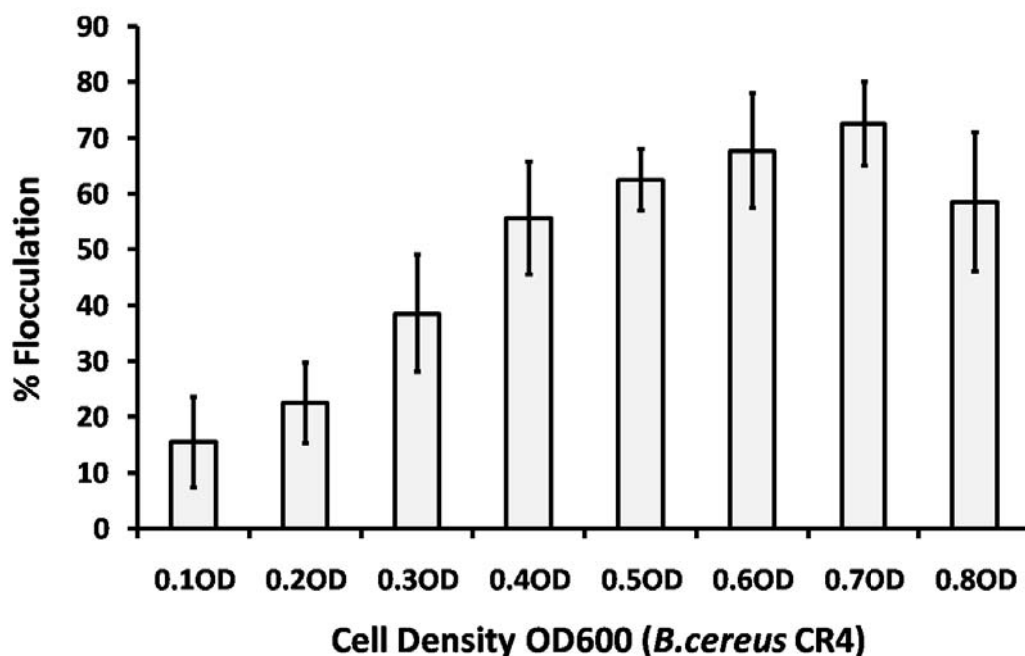


Figure 3. 24 Kaolin Flocculation activity using *B. cereus* CR4 biomass grown in different media



**Figure 3. 25** Effect of cell density of *B. cereus* CR4, (grown in algal media) on flocculation of kaolin.

The density of floc forming bacterial cells play an important role and with an increase in cell density of bacteria, the flocculation of microalgae can be improved. This can be explained by the fact that, increasing the number of cells would provide more amyloids for flocculation. Figure 3.25 shows that the cell density of 0.7OD 600nm of *B.cereus* CR4 was required for 70% flocculation of kaolin. To achieve this cell density during co-cultivation the amount of glucose in the medium and inoculum size must be optimized. Hence optimization was carried out by response surface methodology.

#### **3.2.4.3 Optimization of cocultivation condition for aggregation of *Bacillus* CR4 and *Scenedesmus* sp.**

Based on figure 3.25, with an aim to achieve 70% flocculation the final density of bacterial cells must reach 0.7OD at the time of co-cultivation. To achieve this the central composite design was used to optimize various concentrations of glucose and bacterial inoculum size for optimal growth of microalgae and bacteria. Figure 3.25 alludes that the required cell density of 0.7 OD (600nm) can be achieved at 85mg% glucose with 0.51% initial inoculum of bacteria. However, the presence of glucose did not have any significant effect on the algal growth (Figure 3.26). The growth of *Scenedesmus* sp. indeed decreased from 1.25 OD750nm to 0.63 OD700nm when the bacterial inoculum was increased from 0.15% to 0.86%. Optimal growth of algae can be achieved at 50mg% glucose. Hence glucose concentration of 50mg % glucose was selected for cocultivation and the combined growth of algae and bacteria was checked. The experimental results were in accordance with the predicted values (Figure. 3.27). During cocultivation aggregated growth of algae and bacteria at the respective concentration of glucose was confirmed experimentally (Figure. 3.28).

The cocultivation strategy has been demonstrated to be mutually beneficial as macronutrients and micronutrients are often exchanged between microalgae and bacteria (Scognamiglio *et al.*, 2021). In natural conditions the microalgae and bacteria often show symbiotic relationship where the CO<sub>2</sub> produced by bacteria supports the growth of microalgae while the O<sub>2</sub> produced by microalgeinturn supports the growth of bacteria. Besides gaseous exchange the microalgal culture and bacterial cells growing under cocultivated conditions often alter their individual metabolism to fulfill each others requirement. For example, cocultivation of microalgae with bacteria producing IAA (indole acetic acid) and vitamins have demonstrated the growth of microalgae by several folds (De Bashan *et al.*, 2008). The symbiotic interaction between microalgae and bacteria has been widely documented in case of unicellular microalgae and *Roseobacter* sp (Ravindran *et al.*, 2016).

One of the other strategies in cocultivation involves use of fungi along with microalgae. This method is termed as microalgal cell pelletization. This technique is based on trapping microalgal cells by the growth of fungal hyphae. The charged surface of fungal hyphae can easily interact with the oppositely charged microalgal cells resulting in large pellets or flocs that settles in aggregates. This method has demonstrated about 20% to 30% cost reduction in the final products developed from microalgal biomass. (Ravindran *et al.*, 2016; Moondra *et al.*, 2020).

**Table 3. 19** Optimization of cocultivation conditions for flocculated growth of *Scenedesmus* and *B. cereus* CR4.

Std	Run	Block	Glucose (mg%)	Inoculum (%)	Bacterial growth (OD600)	Algal growth (OD750)
8	1	Block 1	50.0	1.00	0.977	0.059
2	2	Block 1	85.3	0.15	0.274	1.47
3	3	Block 1	14.6	0.86	0.275	0.542
9	4	Block 1	50.0	0.51	0.626	2.5
5	5	Block 1	0.00	0.51	0.001	0.883
6	6	Block 1	100.0	0.51	0.932	0.381
4	7	Block 1	85.3	0.86	0.853	1.2
7	8	Block 1	50.0	0.01	0.034	1.52
1	9	Block 1	14.6	0.15	0.022	0.475

Design-Expert® Software

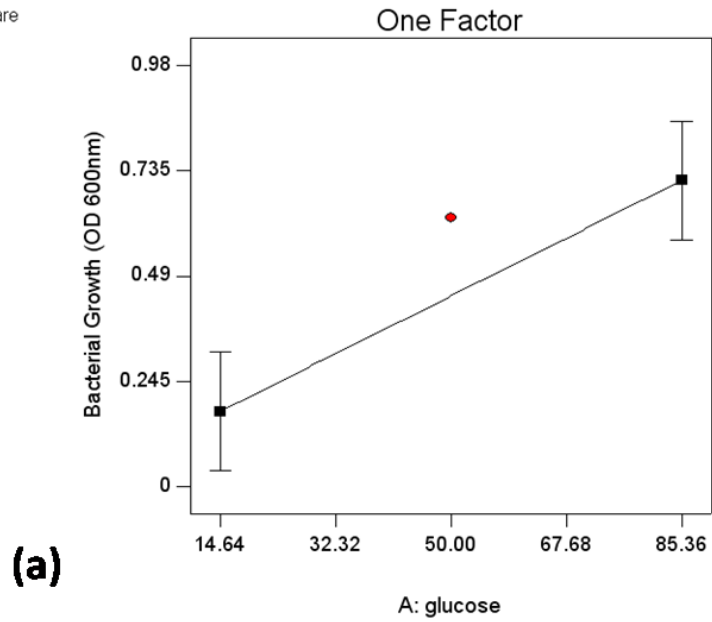
Bacterial Growth

• Design Points

X1 = A: glucose

Actual Factor

B: Inoculum = 0.51



Design-Expert® Software

Bacterial Growth

• Design Points

X1 = B: Inoculum

Actual Factor

A: glucose = 50.00

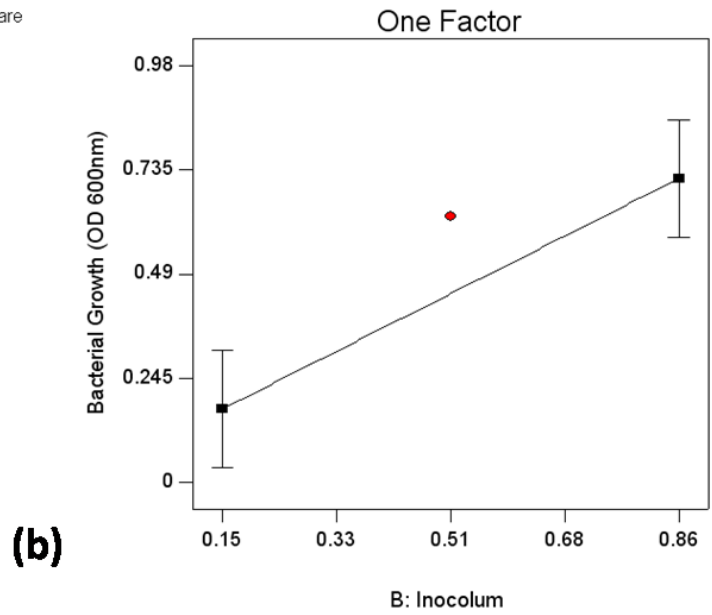


Figure 3. 26 Effect of glucose (a) and inoculum size (b) on growth of *B.cereus* CR4.

Design-Expert® Software

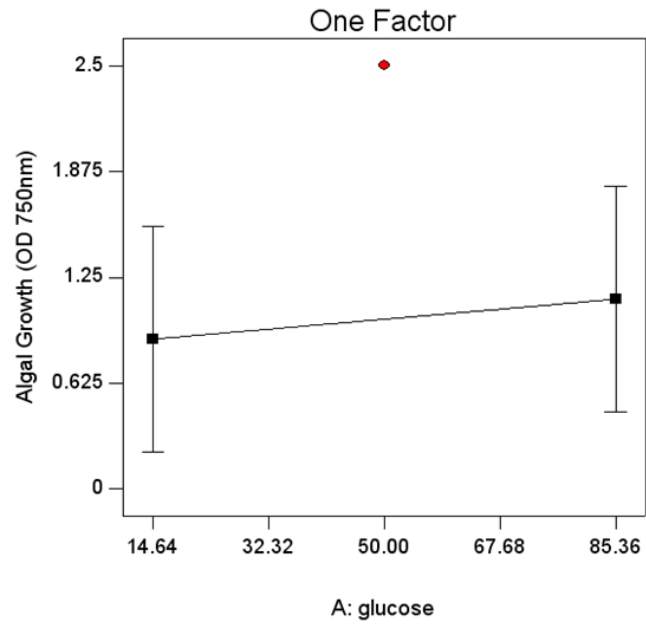
Algal Growth

• Design Points

X1 = A: glucose

Actual Factor

B: Inoculum = 0.51



(a)

Design-Expert® Software

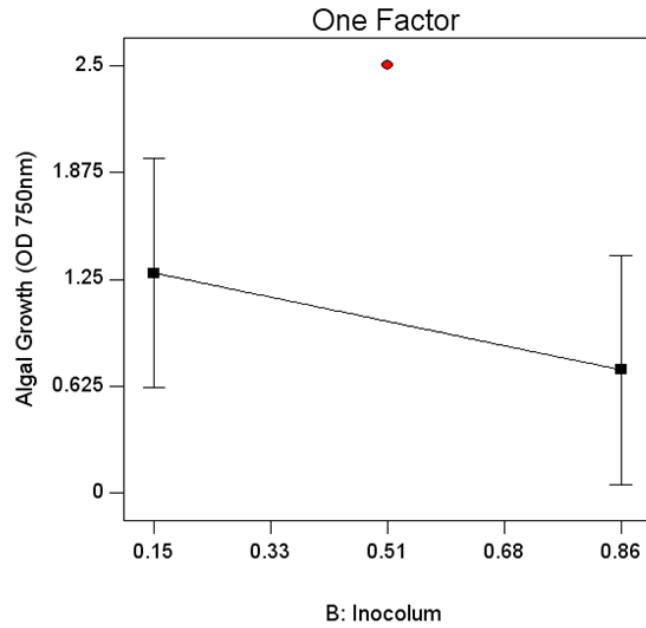
Algal Growth

• Design Points

X1 = B: Inoculum

Actual Factor

A: glucose = 50.00



(b)

Figure 3. 27 Effect of glucose (a) and inoculum size (b) on growth of *Scenedesmus*.

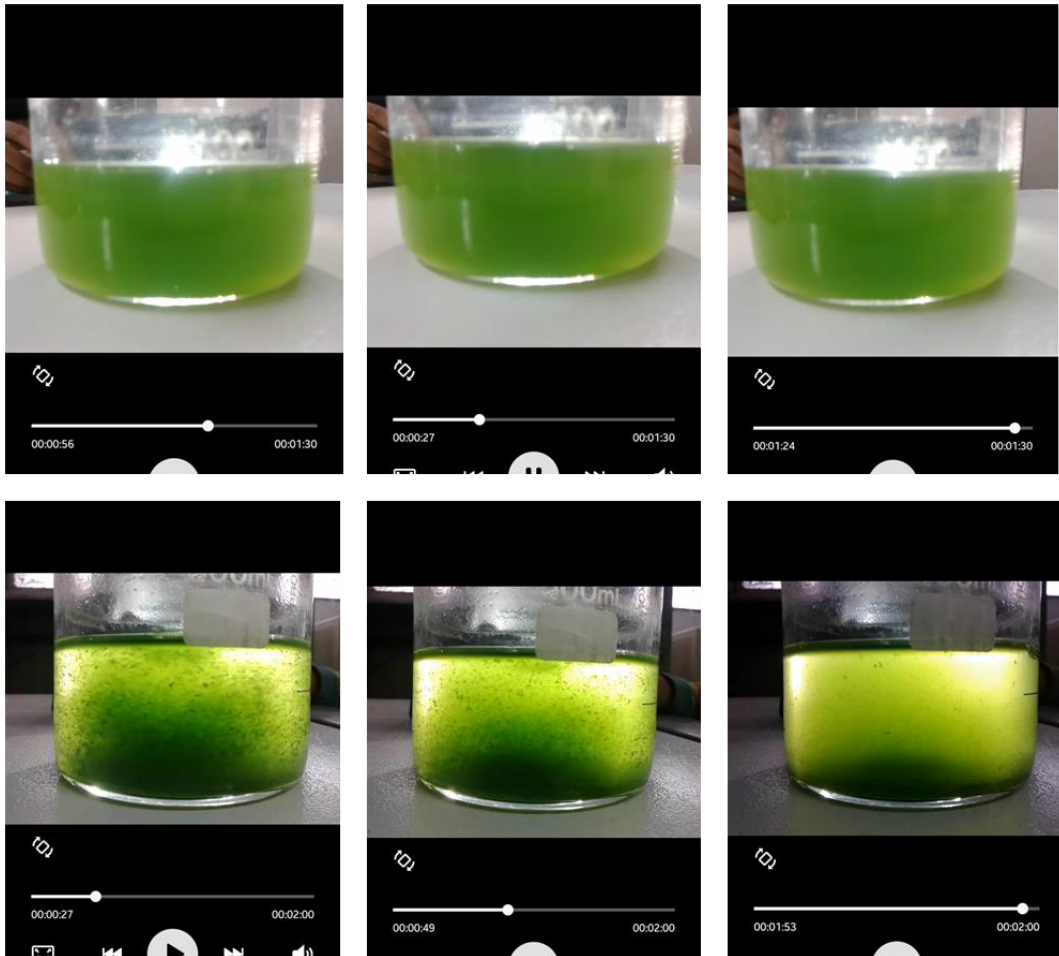


**Figure 3. 28** Cocultivation of *Bacillus* and *Scenedesmus* for aggregated growth.

### **3.2.5 Application of *B. cereus* CR4 in harvest of *Scenedesmus* employed for nutrient removal**

#### **3.2.5.1 Nutrient removal from waste water at bench scale**

Microalgae have been proved to be an excellent resource for the generation of biofuels, biofertilizer, animal fodder as well as a natural cosmetic. The growth and recovery of microalgal biomass must be robust and commercially sustainable. The cultivation of

microalgae in synthetic media can be costly. As microalgae can utilize atmospheric carbon dioxide as a sole source of carbon, they have shown to be an excellent organism for the

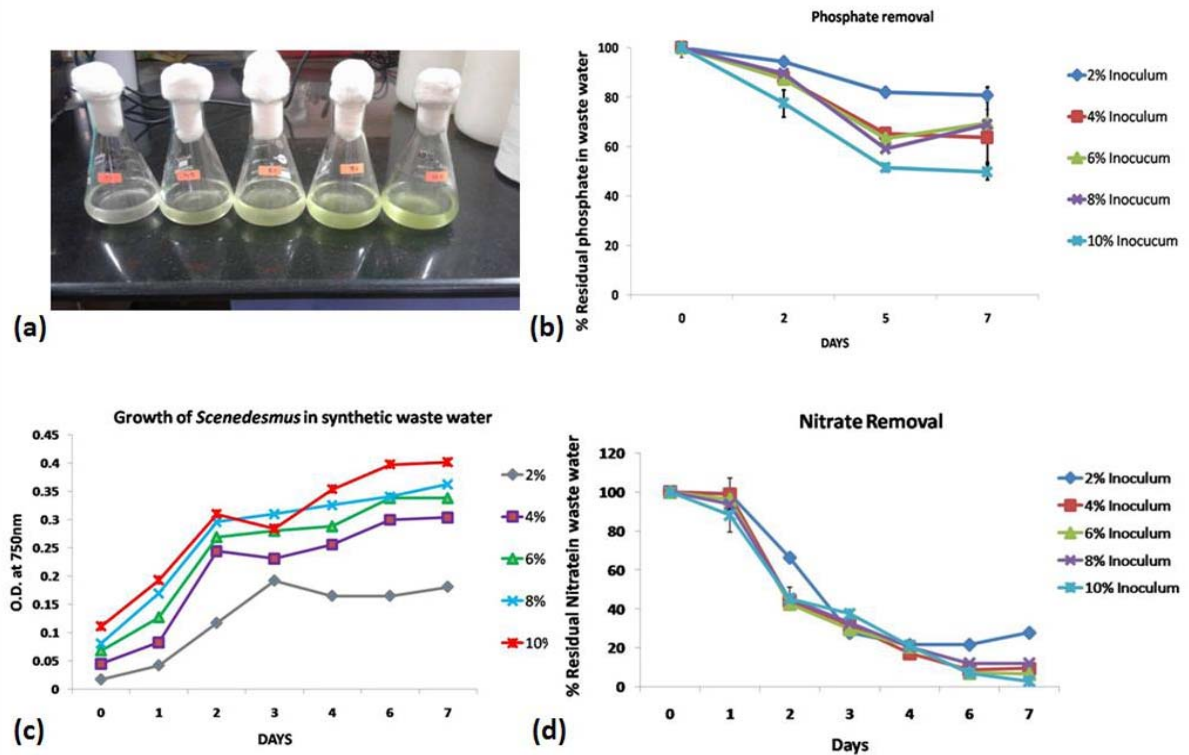


**Figure 3.29** Bench scale studies for nutrient removal from synthetic wastewater. a) Flasks with different inoculum size of microalgae. b) phosphate removal c) growth and d) nitrate removal respectively.

removal of nutrients and bioremediation of metals from waste water (Alvarez-Diaz *et al.*, 2017, Shaid *et al.*, 2019; Mazurkiewicz *et al.*, 2020). On the other hand, domestic waste water that is rich in nitrates, phosphates and various forms of carbon sources has been considered as most suitable alternative for bulk cultivation of microalgae and production of biofuel from the resulting biomass (Schen *et al.*, 2015, wang *et al.*, 2017). Hence it is necessary to develop low cost methods of microalgae cultivation and harvesting (Mohan *et al.*, 2019; Konur *et al.*,

2021). In order to exploit the ability of microalgae to remove phosphates and nitrates from waste water studies were initiated at flask level with synthetic waste water (Figure. 3.29 a). The flasks were inoculated with different inoculum size of *Scenedesmus* sp. followed by estimation of growth, residual nitrate and residual phosphate at regular intervals. There was significant increase in growth of *Scenedesmus* sp. when the inoculum size was increased from 2% to 10% (Figure. 3.29 b). The phosphate removal varied from 20% to 45% depending on the inoculum size (Figure. 3.29 c). Except 2% inoculum size all the flasks demonstrated more than 95% removal of nitrate (Figure. 3.29 d).

### **3.2.5.2 Nutrient removal from waste water at batch reactor level**

Based on flask level studies a batch reactor containing 5L of synthetic waste water was constructed. The bioreactor was inoculated with 10% v/v *Scenedesmus* sp. and the amount of residual nitrate and phosphate was estimated at regular intervals. Within first 24hrs about 60.7% of nitrate and 40.2% of phosphate was removed by the *Scenedesmus* biomass. The rapid uptake of nitrate and phosphate during the first day resulted in sharp increase in the optical density from 0.8 to 1.06 which indicated growth of the microalgal cells. At the end of 48hrs about 99% nitrate (Figure. 3.30a) was removed while the residual phosphate reached 57.1% which means 43.9% removal (Figure. 3.30b). Thereafter the removal of phosphate became stagnant and only 50% of the phosphate was removed at the end of 7 days. A similar observation has been documented by deBashan *et al.*, (2004). The phosphate removal by *Scenedesmus dimorphus* does not exceed by 55%. Besides limiting phosphate removal several documented evidence suggests the role of nitrate to phosphate ratio in phosphate removal from waste water and growth (Lau *et al.*, 1995).

In order to check the effect of nitrate on phosphate removal by *Scenedesmus* sp. a separate experiment was carried out where the synthetic waste water was fortified with nitrate after 48hrs of inoculation. On the third day the removal of nitrate showed a similar trend along with the removal of phosphate. Lee *et al.*, (2015)

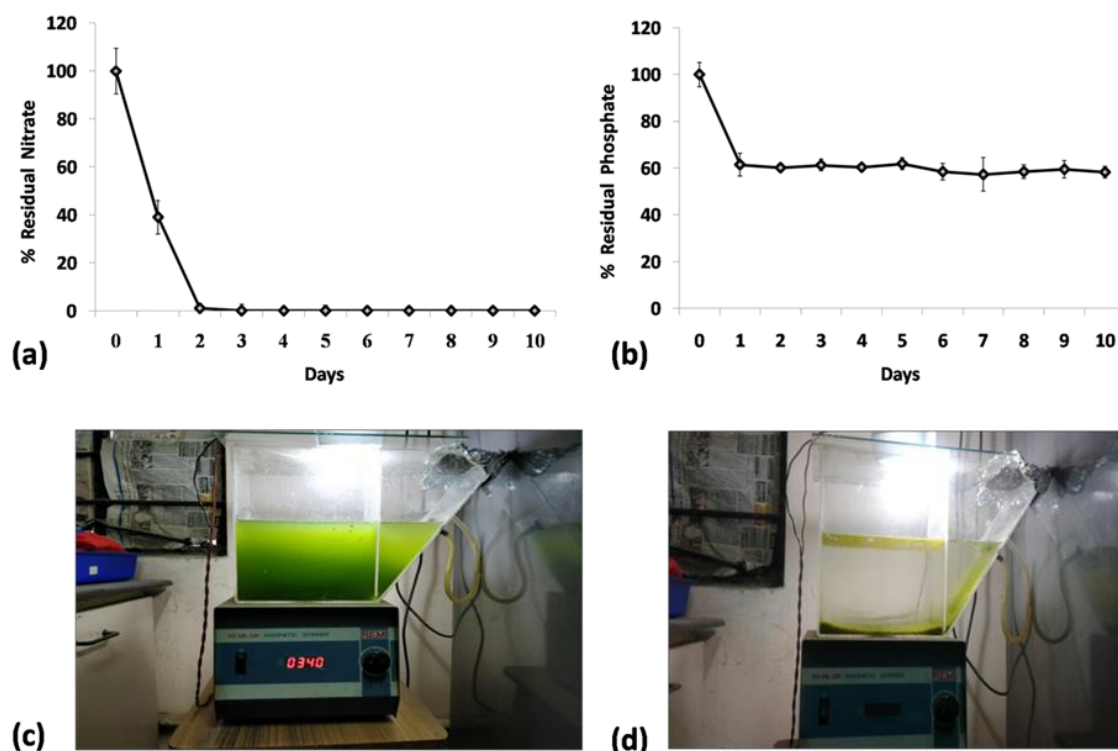


**Figure 3.30** Removal of nitrate and phosphate from synthetic waste water using *Scenedesmus* sp in a batch reactor. a) % residual nitrate after treatment. b) % residual phosphate after treatment. c) Suspended *Scenedesmus* sp. before addition of *B. cereus* CR4. d) Flocculated *Scenedesmus* sp. after addition of *B. cereus* CR4.

have demonstrated effective bioremediation of phosphates and nitrates upto (35-88%) and (43-89%) respectively in lab scale photobioreactor designed for the treatment of municipal waste water. Besides nitrogen, phosphorous is the second most abundant micronutrient, required by the microalgae for its growth. The removal of phosphate by *Scenedesmus* have shown similar trend in other studies (Yewalkar and Kulkarni *et al.*, 2017). The consortia of *B. lichiniiformis* and *Chlorella vulgaris* have demonstrated 88% removal of nitrates and 80% removal of phosphates from synthetic waste water. Besides nutrients removal the

biofloculant nature of *Bacillus lichiniformis* also aids in the aggregation of microalgal cells leading to flocculation and harvesting of microalgal biomass (Ji *et al.*, 2018).

### 3.2.6 Nutrient removal from waste water in continuous reactor

The waste water treatment carried out in domestic and industrial treatment plants is a continuous process. Hence it becomes imperative to scrutinize the nutrient removal from waste water in a continuous setup. The continuous bioreactor was setup with synthetic waste water and evaluated for the nutrient removal using microalgae.



**Figure 3. 31** Continous reactor for the nutrient removal from wastewater.

The use of microalgae for nutrient removal from waste water also offers additional advantage of sequestering of heavy metals from the waste water. This can easily solve the problem of

eutrophication of water bodies caused due to excessive nutrients present in domestic, industrial and agricultural waste water. The growth of microalgae in waste water effluents also reduces the pathogenic coliforms by competitive assimilation of waste water nutrients, making water suitable for discharge in large water bodies. Moreover, the exudates released by microalgae are known to inhibit growth of pathogenic bacteria and fungi which makes them highly suitable for waste water treatment (Ravindran *et al.*, 2016)

### **3.2.6.1 Optimization of flocculation for continuous reactor by response surface methodology**

One of the widely used statistical methods for optimization of parameters for desired response is response surface methodology. The central composite design was employed for the optimization of flow rates for efficient flocculation of microalgae in continuous reactor. In this method the experiments are carried out at five different levels viz. extreme low, low, medium, high and extreme high concentration. The following table represents the values of different flow rates selected for 5 levels respectively.

Synthetic waste water was inoculated with 10% v/v *Scenedesmus* sp. in a continuous bioreactor and the removal of nitrate and phosphate was measured at flow rate of 1 mL/min, 2 mL/min, 4.5 mL/min, 6 mL/min and 8 mL/min. The algal cell density increased from 0.8 O.D to 2.2 O.D at flow rate of 1 mL/min indicating generation of new algal cell and less loss of algal cells in the flow.

On the contrary, the algal cell density decreased to 0.3 O.D. at flow rate of 8 mL/min indicating that the rate of generation of new algal cells was less than the rate of loss of algal cells due to the outflow. Hence, 4.2 mL/min was calculated to be the critical flow rate (Figure. 3.32) i.e., the rate of generation of new algal cells was equal to the loss of algal cells in the flow. At this flow rate the cell density in the bioreactor is supposed to be constant. Estimation of nitrate and phosphate at the test flow rates was carried out. Nitrate removal of 42.95% and phosphate removal of 20.05% was calculated for the critical flow rate 4.2 mL/min.

**Table 3. 20** Optimization of flocculation conditions of the continuous reactor *B. cereus* CR4

Std	Run	Block	Out Flow(ml/min)	Flocculant flow (ml/min)	Flocculation(%)
6	1	Block 1	8.00	4.50	20.5
7	2	Block 1	4.50	1.00	50.6
2	3	Block 1	6.97	2.03	40.6
1	4	Block 1	2.03	2.03	73.9
3	5	Block 1	2.03	6.97	44.7
8	6	Block 1	4.50	8.00	42.9
4	7	Block 1	6.97	6.97	27.1
5	8	Block 1	1.00	4.50	41.5
10	9	Block 1	4.50	4.50	66.9
9	10	Block 1	4.50	4.50	65.6

**Table 3. 21** ANOVA analysis for optimization of flocculation conditions for continuous reactor

Source	Sum of Squares	df	Mean Square	F Value	p-value
Model	2366.16	5	473.23	6.27	0.0499
A-Reactor flow rate	812.01	1	812.01	10.75	0.0305
B-Flocculant flow rate	358.98	1	358.98	4.75	0.0947
AB	61.62	1	61.62	0.82	0.4175
A2	1126.81	1	1126.81	14.92	0.0181
B2	279.91	1	279.91	3.71	0.1265
Residual	302.10	4	75.53		
Lack of Fit	301.26	3	100.42	118.84	0.0673
Pure Error	0.85	1	0.85		
Cor Total	2668.26	9			

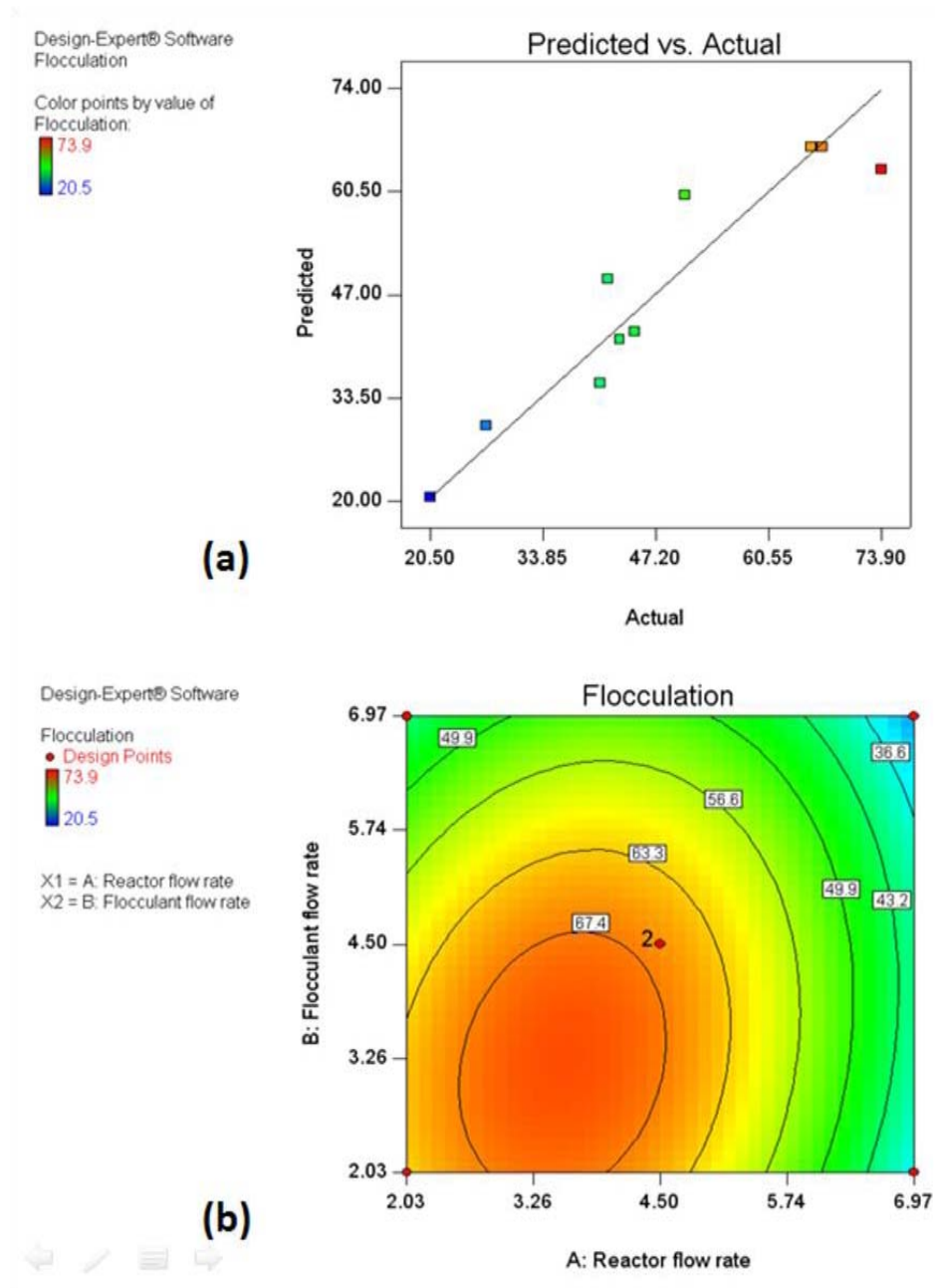


**Figure 3. 32** Optimization of flocculant flow rate and reactor flow rate using central composite design. a) predicted vs actual. b) Contour plot shown effect of flocculant flow rate and reactor outflow rate on flocculation of *Scenedesmus* sp.

The salient results that were discussed in the studies carried out in this chapter are summarized as follows.

- I) *B. cereus* CR4 demonstrated optimal growth at pH 7 and 37°C temperature. Screening of medium components by Plackett Burman method demonstrated significant contribution of lactose, yeast extract and tryptone in production of bioflocculant CR4. Optimization of bioflocculant production by central composite design revealed that use of 0.25% lactose, 0.5% yeast extract and 0.7% tryptone gives maximum bioflocculant production (1.16µg/mg biomass) and maximum flocculation activity of 89.2%
- II) Studies with flocculation of kaolin demonstrates 61% flocculation activity at acidic pH 5 and 60µg/ml of amyloid concentration. Optimization of flocculation conditions for kaolin using central composite design reveals optimum % flocculation of 90% at at pH 3 and 72mg/l amyloid concentration.
- III) Screening of medium components by Plackett Burmann analysis, for optimal growth of *Scenedesmus* sp. revealed significant contribution by NaNO<sub>3</sub> and ZnSO<sub>4</sub> in its growth. Further optimization by central composite design demonstrates 3.46g/l of biomass yield at 125mg% of NaNO<sub>3</sub> and 2.55mg% of ZnSO<sub>4</sub> respectively.
- IV) Under optimized conditions 82.3% flocculation of *Scenedesmus* sp. can be obtained when the pH, biomass and Fe<sup>+3</sup> concentration were adjusted to 4.0, 0.400 (OD 750nm) and 182 mg% respectively.
- V) *Scenedesmus* sp. could remove 99% nitrate and 43.9% phosphate in batch reactor whereas 42.95% nitrate and 20.05% phosphate removal was observed at critical flow rate 4.2 mL/min in continuous reactor.

## References

- Álvarez-Díaz, P. D., Ruiz, J., Arbib, Z., Barragán, J., Garrido-Pérez, M. C. and Perales, J. A. (2017). Freshwater microalgae selection for simultaneous wastewater nutrient removal and lipid production. *Algal Research*, 24, 477-485.
- Arumugam, M., Agarwal, A., Arya, M. C. and Ahmed, Z. (2013). Influence of nitrogen sources on biomass productivity of microalgae *Scenedesmus bijugatus*. *Bioresource technology*, 131, 246-249.
- Bakar, S. N. H. A., Hasan, H. A., Abdullah, S. R. S., Kasan, N. A., Muhamad, M. H. and Kurniawan, S. B. (2021). A review of the production process of bacteria-based polymeric flocculants. *Journal of Water Process Engineering*, 40, 101915.
- De-Bashan, L. E., Antoun, H. and Bashan, Y. (2008). Involvement of Indole 3 acetic acid produced by the growth promoting bacterium *Azospirillum* spp. in promoting growth of *Chlorella vulgaris*. *Journal of Phycology*, 44(4), 938-947.
- De-Bashan, L. E., Hernandez, J. P., Morey, T. and Bashan, Y. (2004). Microalgae growth-promoting bacteria as “helpers” for microalgae: a novel approach for removing ammonium and phosphorus from municipal wastewater. *Water Research*, 38(2), 466-474.
- Duanis-Assaf, D., Steinberg, D., Chai, Y. and Shemesh, M. (2016). The LuxS based quorum sensing governs lactose induced biofilm formation by *Bacillus subtilis*. *Frontiers in microbiology*, 6, 1517.
- Fiske, C. H. and Subbarow, Y. (1925). The colorimetric determination of phosphorus. *Journal of Biological Chemistry* 66(2), 375-400.
- Follett, M. J. and Ratcliff, P. W. (1963). Determination of nitrite and nitrate in meat products. *Journal of the Science of Food and Agriculture*, 14(3), 138-144.
- Ji, X., Jiang, M., Zhang, J., Jiang, X. and Zheng, Z. (2018). The interactions of algae-bacteria symbiotic system and its effects on nutrients removal from synthetic wastewater. *Bioresource technology*, 247, 44-50.

Konur, O. (2021). Algal biomass production in wastewaters for biodiesel production: A review of the research. *Biodiesel Fuels Based on Edible and Nonedible Feedstocks, Wastes, and Algae*, 719-740.

Lau, P. S., Tam, N. F. Y. and Wong, Y. S. (1995). Effect of algal density on nutrient removal from primary settled wastewater. *Environmental Pollution*, 89(1), 59-66.

Lee, C. S., Lee, S. A., Ko, S. R., Oh, H. M. and Ahn, C. Y. (2015). Effects of photoperiod on nutrient removal, biomass production, and algal-bacterial population dynamics in lab-scale photobioreactors treating municipal wastewater. *Water research*, 68, 680-691.

Lowry, O. H., Rosebrough, N. J., Farr, A. L., and Randall, R. J. (1951) Protein measurement with the Folin phenol reagent. *J. Biol. Chem.* **193**, 265–275.

Mohan, S. V., Dahiya, S., Amulya, K., Katakajwala, R. and Vanitha, T. K. (2019). Can circular bioeconomy be fueled by waste biorefineries—A closer look. *Bioresource Technology Reports*, 7, 100277.

Moondra, N., Jariwala, N. D., and Christian, R. A. (2020). Microalgal-bacterial consortia: an alluring and novel approach for domestic wastewater treatment. *WCM*, 4, 51-56.

Mazurkiewicz, J., Mazur, A., Mazur, R., Chmielowski, K., Czekala, W., and Janczak, D. (2020). The Process of Microbiological Remediation of the Polluted Słoneczko Reservoir in Poland: For Reduction of Water Pollution and Nutrients Management. *Water*, 12(11), 3002

Ni, Z., Wu, X., Li, L., Lv, Z., Zhang, Z., Hao, A. and Li, C. (2018). Pollution control and in situ bioremediation for lake aquaculture using an ecological dam. *Journal of Cleaner Production*, 172, 2256-2265.

Okaiyeto, K., Nwodo, U. U., Okoli, S. A., Mabinya, L. V. and Okoh, A. I. (2016). Implications for public health demands alternatives to inorganic and synthetic flocculants: bioflocculants as important candidates. *Microbiology Open*, 5(2), 177-211.

Podevin, M., De Francisci, D., Holdt, S. L. and Angelidaki, I. (2015). Effect of nitrogen source and acclimatization on specific growth rates of microalgae determined by a high-throughput in vivo microplate autofluorescence method. *Journal of Applied Phycology*, 27(4), 1415-1423.

Ravindran, B., Gupta, S. K., Cho, W. M., Kim, J. K., Lee, S. R., Jeong, K. H. and Choi, H. C. (2016). Microalgae potential and multiple roles—current progress and future prospects—an overview. *Sustainability*, 8(12), 1215.

Scognamiglio, V., Giardi, M. T., Zappi, D., Touloupakis, E., and Antonacci, A. (2021). Photoautotrophs–Bacteria Co-Cultures: Advances, Challenges and Applications. *Materials*, 14(11), 3027.

Shahid, A., Ishfaq, M., Ahmad, M. S., Malik, S., Farooq, M., Hui, Z. and Mehmood, M. A. (2019). Bioenergy potential of the residual microalgal biomass produced in city wastewater assessed through pyrolysis, kinetics and thermodynamics study to design algal biorefinery. *Bioresource technology*, 289, 121701.

Shen, Q. H., Jiang, J. W., Chen, L. P., Cheng, L. H., Xu, X. H. and Chen, H. L. (2015). Effect of carbon source on biomass growth and nutrients removal of *Scenedesmus obliquus* for wastewater advanced treatment and lipid production. *Bioresource technology*, 190, 257-263.

Vandamme, D., Foubert, I. and Muylaert, K. (2013). Flocculation as a low-cost method for harvesting microalgae for bulk biomass production. *Trends in biotechnology*, 31(4), 233-239.

Volland, S., Bayer, E., Baumgartner, V., Andosch, A., Lütz, C., Sima, E. and Lütz-Meindl, U. (2014). Rescue of heavy metal effects on cell physiology of the algal model system *Micrasterias* by divalent ions. *Journal of Plant Physiology*, 171(2), 154-163.

Wang, Y., Ho, S. H., Cheng, C. L., Nagarajan, D., Guo, W. Q., Lin, C. and Chang, J. S. (2017). Nutrients and COD removal of swine wastewater with an isolated microalgal strain *Neochloris aquatica* CL-M1 accumulating high carbohydrate content used for biobutanol production. *Bioresource technology*, 242, 7-14.

Xiong, Y., Wang, Y., Yu, Y., Li, Q., Wang, H., Chen, R. and He, N. (2010). Production and characterization of a novel bioflocculant from *Bacillus licheniformis*. *Applied and environmental microbiology*, 76(9), 2778-2782.

Yewalkar-Kulkarni, S., Gera, G., Nene, S., Pandare, K., Kulkarni, B. and Kamble, S. (2017). Exploiting phosphate-starved cells of *Scenedesmus* sp. for the treatment of raw sewage. *Indian journal of microbiology*, 57(2), 241-249.